Electronic Supplementary Material (ESI) for Physical Chemistry Chemical Physics.
This journal is © the Owner Societies 2024

Supporting Information

Temperature-dependent NIR-CPL spectra of chiral Yb(III) complexes

*Annika Sickinger,[#,‡] Maxime Grasser,[ǁ,‡] Bruno Baguenard,[‡] Amina Bensalah-Ledoux,[‡] Laure Guy,[#] Anh Thy Bui,[#,¤] Yannick Guyot,[‡] Vincent Dorcet,[ǁ] Fabrice Pointillart,[ǁ] Olivier Cador,[ǁ] Stéphan Guy,[‡] Olivier Maury,[#] Boris Le Guennic,[ǁ] François Riobé.[#,§]**

Univ. Lyon, ENS de Lyon, CNRS, Laboratoire de Chimie UMR 5182, F-69342 Lyon, France.

ǁ Univ. Rennes, CNRS, ISCR (Institut des Sciences Chimiques de Rennes) UMR 6226, F-35000 Rennes, France.

‡ Univ. Lyon, CNRS, Institut Lumière Matière UMR 5306, F-69622 Villeurbanne, France.

¤ Univ. Bordeaux, CNRS, Bordeaux INP, ISM, UMR 5255, F-33400 Talence, France.

§ Univ. Bordeaux, CNRS, Bordeaux INP, ICMCB UMR 5026, F-33600 Pessac, France.

Contents

S 1. MATERIALS AND GENERAL CONSIDERATIONS

Unless stated otherwise, all reactions of air- and/or water-sensitive compounds were carried out under inert gas atmosphere using standard Schlenk techniques.

Solvents were purchased from Fisher Scientific, VWR Chemicals or Carlo Erba Reagents and used without further purification. Acetonitrile, tetrahydrofurane as well as the methanol/dichloromethane mixture used for the complex synthesis were stored over 3 Å molecular sieve. $CDCl_3$ and methanol-d_4 was supplied by Eurisotop. **Starting materials** were purchased from Sigma-Aldrich, TCI, Alfa Aesar or Acros Organics. Poly(dimethylsiloxane) (PDMS) samples were prepared using a two-component Sylgard 184 silicone elastomer kit, supplied by Dow Corning.

Column chromatography was performed using silica gel (40-63 µm) from VWR Chemicals. **Centrifugation** was carried out on a Sigma 2-16P centrifuge (9000 rpm, 10 minutes).

S 2. ANALYTICAL METHODS AND TECHNIQUES

^{1}H, ^{13}C and the corresponding two-dimensional **nuclear magnetic resonance (NMR)** spectra were recorded at room temperature on a Bruker Avance III 300 or on a Bruker Ascend 400 spectrometer. The chemical shifts in ppm were referenced to the solvent residual proton signals ($CDCl_3$: 7.26 ppm; CD_3OD: 3.31 ppm). The multiplicities of the signals were abbreviated as follows: s (singlet), d (doublet), t (triplet), q (quartet), quint (quintet), dd (doublet of doublets), m (multiplet) and br (broad signal).

Acquisition of **low-resolution mass spectra** was performed on an Agilent LCMS 6120, composed of a quadrupole multimode source (ESI + APCI) connected to a HPLC system with a UV/vis detector, operating by an array of diodes. **High resolution mass spectra** were recorded at the Centre Commun de Spectrométrie de Masse (Villeurbanne, France). **Fourier-transform Infrared (FTIR) spectroscopy** was performed using a Perkin Elmer Spectrum 65 device, equipped with an Attenuated Total Reflectance (ATR) module.

Single crystal X-ray diffraction. Single crystals of [Yb(*R,R*-L)$_3$(OTf)$_3$] and [Yb(*S,S*-L)$_3$(OTf)$_3$] were mounted on a D8 VENTURE Bruker-AXS diffractometer for data collection (MoK_α radiation source, λ = 0.71073 Å), from the Centre de Diffractométrie X (CDIFX), Université de Rennes, France. Structures were solved with a direct method using the SHELXT program (and refined with a full matrix least-squares method on F^2 using the SHELXL-14/7 program.[1,2] SQUEEZE procedure of PLATON[3] was performed for structures containing large solvent accessible voids in which residual peak of diffraction were observed. Crystallographic data are summarized in Table S1. Complete crystal structure results as CIF files (CCDC 2245303 for **Δ-Yb** and 2245302 for **Λ-Yb**) including bond lengths, angles, and atomic coordinates are deposited as Supporting Information.

Absorption spectra were recorded on a JASCO V-650 spectrophotometer using complex solutions ($c \approx 10^{-5}$ to 10^{-6} M for absorption in the UV/vis region, optical density < 1) in spectroscopic grade methanol or ethanol using 10x10 mm quartz glass cuvettes. Absorption in the NIR wavelength region was measured using solutions of higher concentrations ($c \approx 10^{-4}$). Measurements of **circular dichroism** in the UV/vis region were performed on a JASCO J-710 spectropolarimeter on complex solutions with concentrations around 10^{-4} to 10^{-5} M.

Luminescence spectra were recorded on a Horiba Jobin Yvon Fluorolog spectrofluorimeter, equipped with a three slit double grating excitation and emission monochromator, the former with a dispersion of 2100 grooves/mm. For the measurement of Yb emission in the NIR wavelength region, an emission grating of 600 grooves/mm with a blaze wavelength of 1000 nm was chosen. The steady-state luminescence was excited by unpolarized light from a 450 W xenon continuous wave (CW) lamp and detected at an angle of 90° using a liquid nitrogen cooled Symphony II FIOE scientific CCD camera. Spectra were reference-corrected for the emission spectral response (detector and grating). Luminescence measurements were conducted on EPR glass tubes containing the complex either as solid powder or dissolved in a mixture of ethanol/methanol in a 4:1 ratio. For measurements at 77 K the sample was cooled by immersion of the EPR tube in liquid nitrogen using a transparent Dewar-type glass tube.

For luminescence lifetimes, the sample in an EPR quartz tube was excited using a pulsed Nd:YAG laser (SpectraPhysics), operating at 10 Hz. Light emitted at right angles to the excitation beam was focused onto the slits of a monochromator (PTI120), which was used to select the appropriate wavelength (400 nm). The growth and decay of the luminescence at selected wavelengths was detected using a Ge photodiode (Edinburgh Instruments, EI-P) and recorded using a digital oscilloscope (Tektronix TDS320) before being transferred for analysis. Luminescence lifetimes were obtained by iterative reconvolution of the detector response (obtained by using a scatterer) with exponential components for growth and decay of the metal-centered luminescence.

NIR-CD UV absorption and CD measurements were performed on a homemade CD spectrometer depicted in Fig.1. It is based on the standard CD scheme described elsewhere.[4] The light source is constituted of an UV 150W xenon lamp from Oriel followed by a Digikrom CM112 double monochromator (slit bandwidth:1nm). A Rochon prism and a Hinds Photo-Elastic Modulator (PEM) driven at 50kHz modulate the beam polarization through all ellipticities from left- circular, to elliptical, to linear, to right-circular polarization. After passing perpendicularly through the thin film, the light is detected with an R14773

Hamamatsu photomultiplier tube. The CD is the ratio of the DC over the AC components of the signal. The DC and AC parts of the signal are measured with a multimeter (Keythley M2000) and a lock-in amplifier (Standford SR830) phase-locked with the PEM, respectively. The computer controls the light wavelength, the PEM phase retardation, and records the AC and DC signals.

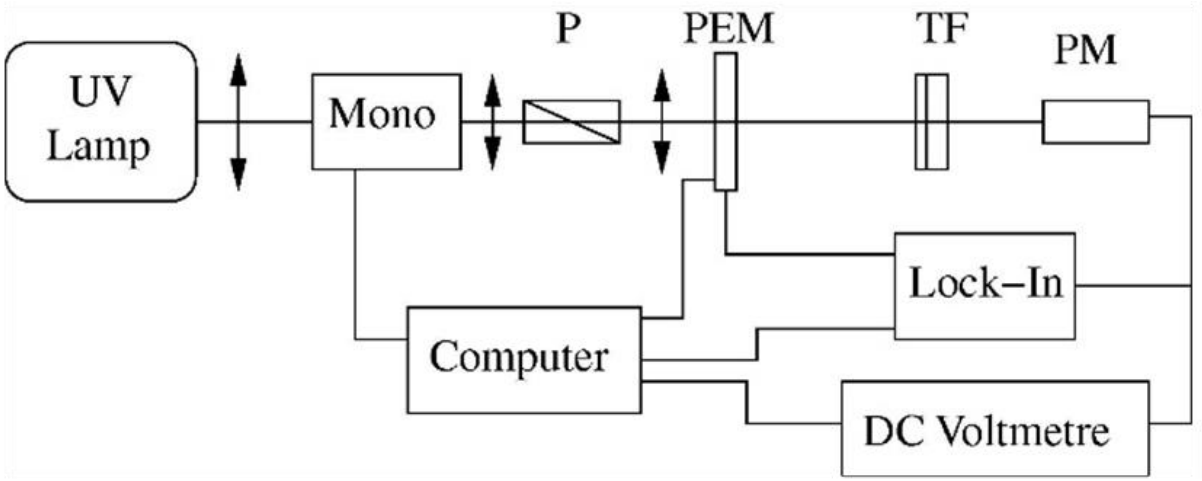

Figure S1: *CD spectrometer: Mono, monochromator; P, Rochon linear polarizer; PEM,photoelastic modulator; TF, thin film sample; PM, photomultiplier*

NIR CPL set-up. NIR CPL spectra are recorded on a homemade apparatus displayed in Figure S1. Solutions in quartz cuvette are excited at 365 nm by a laser diode (Roithner Lasertechnik GmbH, model: UVLED365-11E, FWHM: 12 nm; optical output power: 4 mW). The fluorescence is collected with a lens and separated by means of a λ/4 waveplate (45°) and a polarizing beam splitter. With this arrangement, the light is split into two components of either left- or right-circularly polarized light. Each arm is further imaged on one side of a fiber bundle. The other extremity of the bundle is focused at the entrance slit of a spectrophotometer. The light spectrally separated is imaged on a CCD camera. The “upper/lower” part of the camera record the left- or right-handed circularly polarized spectra. Because of the brightness of the molecules as well as their high glum, this set-up allows a fast record of the CPL spectra in less than one second. However, the silicon detector cut-off prevents for recording at wavelengths longer than 1050 nm. We also used standard set-up using the PEM/locking detection scheme with an IR photo-multiplier or Si detector for CPL and ECD measurements, respectively. This set-up has already been described in former articles.[5–7]

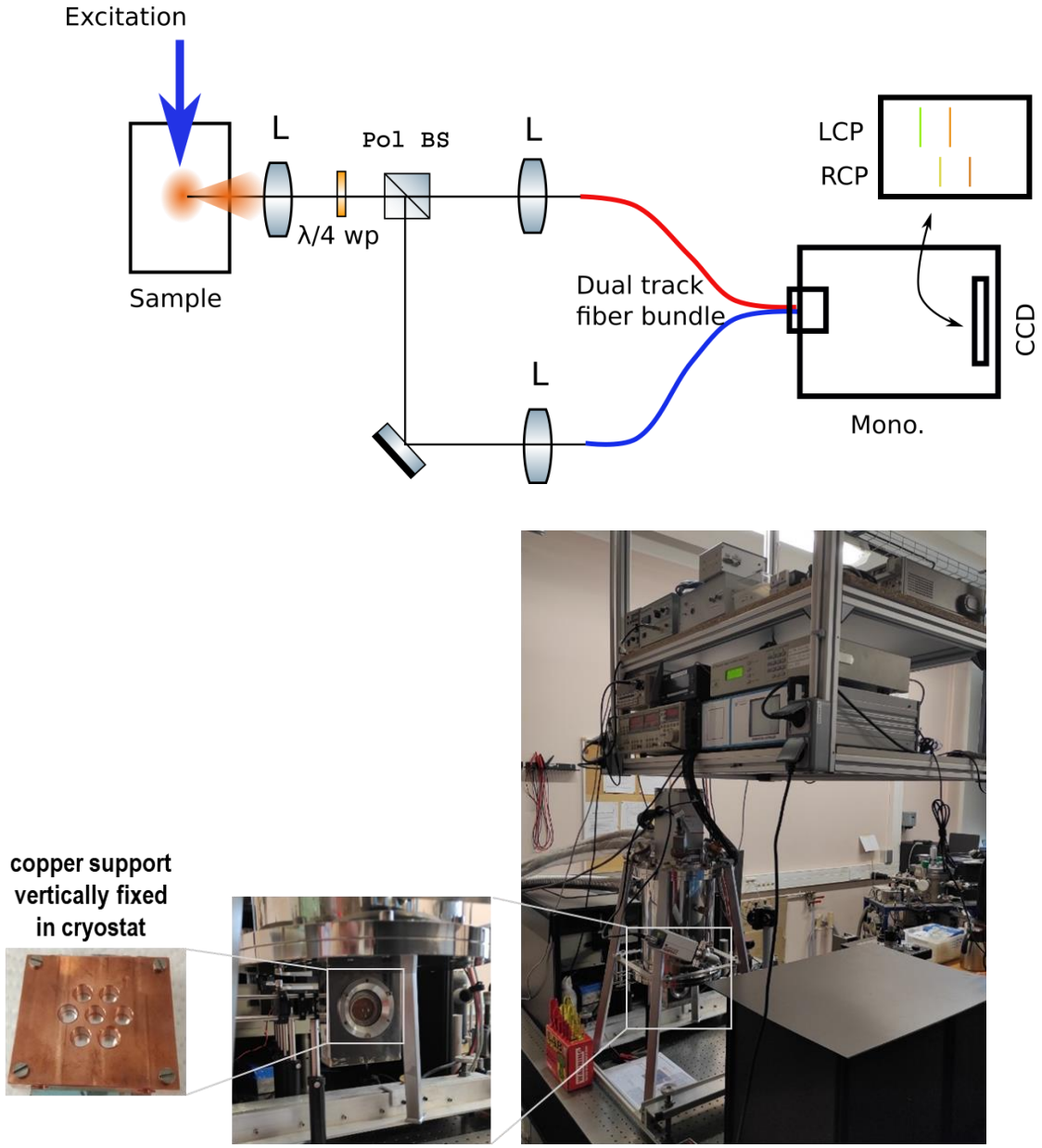

Figure S2: *(Up) Schematic representation of the NIR-CPL (BS+CCD) based setup. L: lenses; λ/4 wp: λ/4 waveplates; BS: polarizer beam splitter; Mono: monochromator. (Bottom) Picture of the cryostat in the set-up and of the sample holder.*

S 3. LIGAND SYNTHESES

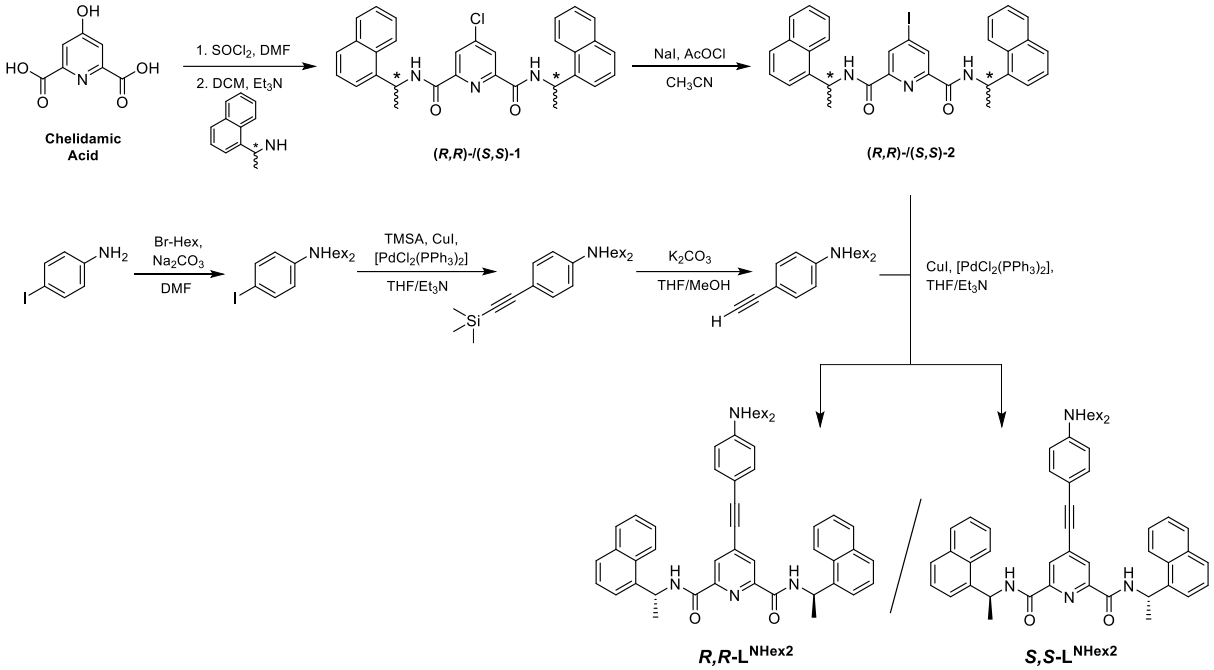

Scheme S1: *Synthetic pathway towards the chiral ligands R,R-LNHex2 and S,S-LNHex2 bearing conjugated antenna functionalities, starting from chelidamic acid.*

SYNTHESIS OF (*R,R*)-1/(*S,S*)-1[8]

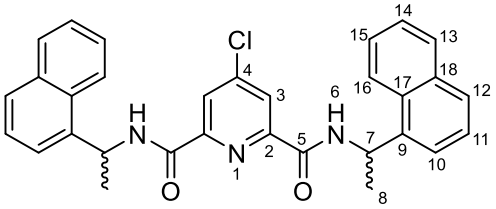

$C_{31}H_{26}ClN_3O_2$
508.02 g/mol

Under argon atmosphere, chelidamic acid (500 mg, 2.49 mmol, 1 equiv.) was suspended in thionyl chloride (50 mL) and the suspension was cooled to 0°C using an ice/water bath. Anhydrous DMF (0.3 mL) was added and the mixture was stirred at 80°C overnight. The solvent was co-evaporated with two portions of toluene (2 x 10 mL) and the remaining solid was dissolved in dichloromethane (10 mL) under argon atmosphere. The solution was cooled to 0°C and the chiral enantiopure (*R*)-(+)- or (*S*)-(-)-1-(1-naphthyl)ethylamine (1.06 g, 6.22 mmol, 2.5 equiv.), dissolved in Et_3N (1 mL, 7.97 mmol, 3.2 equiv.), was slowly added. The orange mixture was stirred at room temperature overnight. A 1 M aqueous solution of K_2CO_3 was added until pH = 10 and the organic phase was washed with water (twice) and with brine, dried over anhydrous magnesium sulfate and the solvent was evaporated under reduced pressure. The crude product was purified by flash chromatography (Al_2O_3 activity III, dichloromethane/ethyl acetate 98:2) to yield both the enantiomer products as a white solid (0.88 g, 1.74 mmol, 70%).

^{1}H-NMR (300 MHz, $CDCl_3$, 25 °C): δ [ppm] = 8.29 (s, 2H, H-3), 8.12-8.07 (m, 2H, H-16), 7.89-7.84 (m, 2H, H-13), 7.82-7.77 (m, 2H, H-12), 7.74 (d, $^{3}J_{HH}$ = 8.5 Hz, 2H, H-6), 7.53-7.47 (m, 4H, H-14, H-15), 7.41-7.38 (m, 4H, H-10, H-11), 6.03-5.93 (m, 2H, H-7), 1.61 (d, $^{3}J_{HH}$ = 6.8 Hz, 6H, H-8).

^{13}C-NMR (75 MHz, $CDCl_3$, 25 °C): δ [ppm] = 161.5 (C-5), 150.2 (C-2), 147.8 (C-4), 138.0(C-9), 134.1 (C-18), 131.1 (C-17), 129.1 (C-13), 128.7 (C-12), 126.9 (C-15), 126.1 (C-14), 125.7 (C-3), 125.4 (C-11), 123.3 (C-16), 122.9 (C-10), 45.5 (C-7), 21.0 (C-8).

HRMS (ESI): found 508.1783 m/z $[M+H]^+$, calculated for $C_{31}H_{26}ClN_3O_2$ 508.1786 m/z.

SYNTHESIS OF (*R,R*)-2/(*S,S*)-2[8]

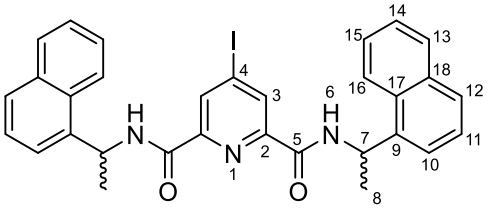

$C_{31}H_{26}IN_3O_2$
599.47 g/mol

A suspension of **(*R,R*)-1** or **(*S,S*)-1** (400 mg, 0.77 mmol, 1 equiv.) and sodium iodide (1.20 g, 7.68 mmol, 10 equiv.) in acetonitrile (50 mL) was sonicated for 1 h in an ultrasound bath. Acetyl chloride (450 µL, 6.3 mmol, 8 equiv.) was added dropwise and the mixture was sonicated for further 2 h. Dichloromethane (50 mL) was added to the suspension and the organic phase was washed with an aqueous saturated Na_2CO_3 solution, a 0.1 M aqueous solution of sodium thiosulfate, water (until pH = 7) and brine. The solution was dried with anhydrous Na_2SO_4 and the solvent was evaporated. After recrystallization of the crude product from hot methanol, the both product enantiomers **(*R,R*)-2** and **(*S,S*)-2** were obtained as white solids in yields of 70-75%.

^{1}H-NMR (300 MHz, $CDCl_3$, 25 °C): δ [ppm] = 8.70 (s, 2H, H-3), 8.14-8.08 (m, 2H, H-16), 7.92-7.86 (m, 2H, H-13), 7.83 (dd, $^{3}J_{HH}$ = 6.9 Hz, $^{4}J_{HH}$ = 2.4 Hz, 2H, H-12), 7.63 (d, $^{3}J_{HH}$ = 8.4 Hz, 2H, H-6), 7.54-7.48 (m, 4H, H-14, H-15), 7.45-7.39 (m, 4H, H-10, H-11), 6.05-5.95 (m, 2H, H-7), 1.64 (d, $^{3}J_{HH}$ = 6.7 Hz, 6H, H-8).

^{13}C-NMR (75 MHz, $CDCl_3$, 25 °C): δ [ppm] = 161.3 (C-5), 148.9 (C-2), 138.0 (C-9), 134.7 (C-3), 134.1 (C-18), 131.1 (C-17), 129.1 (C-13), 128.8 (C-12), 126.9 (C-15), 126.2 (C-14), 125.4 (C-11), 123.4 (C-16), 122.9 (C-10), 107.4 (C-4), 45.5 (C-7), 21.0 (C-8).

HMRS (ESI): found 600.1143 m/z $[M+H]^+$, calculated for $C_{31}H_{26}IN_3O_2$ 600.1142 m/z.

SYNTHESIS OF 4-IODO-*N,N*-DIHEXYLANILINE[9]

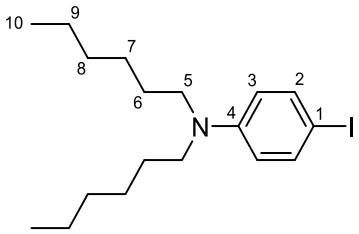

$C_{18}H_{30}IN$
387.35 g/mol

4-Iodoaniline (1.00 g, 4.57 mmol, 1 equiv.) and 1-bromohexane (2.2 mL, 15.54 mmol, 3.4 equiv.) were dissolved in DMF (25 mL) and sodium iodide (2.74 g, 18.28 mmol, 4 equiv.) and sodium carbonate (0.87 g, 8.23 mmol, 1.8 equiv.) were added. The mixture was stirred at 120 °C for 24 h. Deionized water was added and the aqueous phase was extracted with ethyl acetate. The combined organic layers were washed with water and brine, dried over Na_2SO_4 and the solvent was evaporated. The crude product was purified by column chromatography (SiO_2, pentane/DCM: 8/1) to yield 4-iodo-*N,N*-dihexylaniline as a colorless oil (0.87 g, 2.23 mmol, 49%).

^{1}H-NMR (300 MHz, $CDCl_3$, 25 °C): δ [ppm] = 7.43 (d, $^3J_{HH}$ = 9.1 Hz, 2H, H-2), 6.43 (d, $^3J_{HH}$ = 9.1 Hz, 2H, H-3), 3.24 (t, $^3J_{HH}$ = 7.6 Hz, 4H, H-5), 1.63-1.52 (m, 4H, H-6), 1.39-1.29 (m, 12H, H-7, H-8, H-9), 0.93 (t, $^3J_{HH}$ = 6.7 Hz, 6H, H-10).

SYNTHESIS OF 4-(TRIMETHYLSILYLETHYNYL)-*N,N*-DIHEXYLANILINE

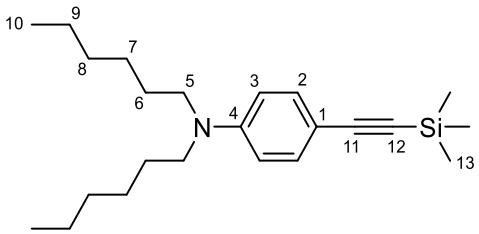

$C_{23}H_{39}NSi$
357.66 g/mol

Under argon atmosphere, 4-iodo-*N,N*-dihexylaniline (1.80 g, 4.65 mmol, 1 equiv.) was dissolved in a mixture of tetrahydrofuran (20 mL) and Et_3N (15 mL). The solution was degassed by sparging with argon for 30 min, followed by the addition of copper iodide (0.17 g, 0.93 mmol, 0.2 equiv.), [$PdCl_2(PPh_3)_2$] (0.32 g, 0.46 mmol, 0.1 equiv.) and ethynyltrimethylsilane (1.3 mL, 9.30 mmol, 2 equiv.). The mixture was stirred overnight at room temperature. Dichloromethane and deionized water were added, the aqueous phase was extracted with dichloromethane and the combined organic layers were washed with water and brine and dried over Na_2SO_4. After evaporation of the solvent, the crude product was purified by column chromatography (SiO_2, pentane/DCM: 8/1) to yield 4-(trimethylsilylethynyl)-*N,N*-dihexylaniline as yellow oil (1.37 g, 3.82 mmol, 82%).

^{1}H-NMR (300 MHz, $CDCl_3$, 25 °C): δ [ppm] = 7.29 (d, $^3J_{HH}$ = 9.0 Hz, 2H, H-2), 6.50 (d, $^3J_{HH}$ = 9.0 Hz, 2H, H-3), 3.25 (t, $^3J_{HH}$ = 7.6 Hz, 4H, H-5), 1.60-1.50 (m, 4H, H-6), 1.36-1.26 (m, 12H, H-7, H-8, H-9), 0.90 (t, $^3J_{HH}$ = 6.7 Hz, 6H, H-10), 0.23 (s, 12H, H-13).

SYNTHESIS OF 4-ETHYNYL-*N,N*-DIHEXYLANILINE

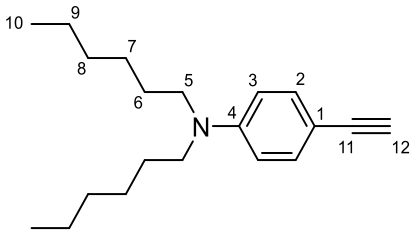

$C_{20}H_{31}N$
285.48 g/mol

4-(Trimethylsilylethynyl)-*N,N*-dihexylaniline (0.50 g, 1.40 mmol, 1 equiv.) was dissolved in a mixture of THF (10 mL) and methanol (10 mL). K_2CO_3 (0.38 g, 2.80 mmol, 2 equiv.) was added and the suspension was stirred for 1 h at room temperature, before it was diluted with dichloromethane, filtered and concentrated under reduced pressure. The remaining solid was purified by filtration over a silica plug with dichloromethane as eluent. After solvent removal, 4-ethynyl-*N,N*-dihexylaniline was obtained as a yellow oil in quantitative yields.

^{1}H-NMR (300 MHz, $CDCl_3$, 25 °C): δ [ppm] = 7.32 (d, $^3J_{HH}$ = 8.9 Hz, 2H, H-2) 6.53 (d, $^3J_{HH}$ = 8.9 Hz, 2H, H-3), 3.26 (t, $^3J_{HH}$ = 7.8 Hz, 4H, H-5), 2.96 (s, 1H, H-12), 1.62-1.52 (m, 4H, H-6), 1.36-1.28 (m, 12H, H-7, H-8, H-9), 0.91 (t, $^3J_{HH}$ = 6.5 Hz, 6H, H-10).

SYNTHESIS OF LIGANDS (*R,R*)-L^{NHex2} and (*S,S*)-L^{NHex2}

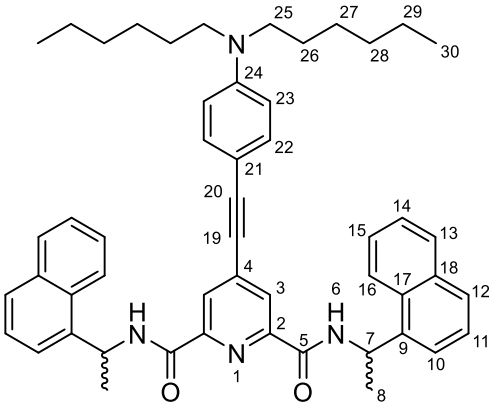

$C_{51}H_{56}N_4O_2$
757.04 g/mol

Under argon atmosphere, a solution of **(*R,R*)-2** or **(*S,S*)-2** (200 mg, 333 mmol, 1 equiv.) in dry tetrahydrofuran was degassed by sparging with argon for 30 min. Copper iodide (13 mg, 66 µmol, 0.2 equiv.), $[PdCl_2(PPh_3)_2]$ (23 mg, 33 µmol, 0.1 equiv.) and a solution of 4-ethynyl-*N,N*-dihexylaniline (143 mg, 500 µmol, 1.5 equiv.) in Et_3N (8 mL) was added. The mixture was stirred for 24 h at room temperature, before it was diluted with dichloromethane. The organic solution was washed with saturated, aqueous NH_4Cl solution, water and brine, dried over Na_2SO_4 and the solvent was evaporated under reduced pressure. The crude product was purified by column chromatography (SiO_2, DCM) to yield the desired ligands as orange solid.

(*R,R*)-L^{NHex2}: 74% yield

^{1}H-NMR (400 MHz, $CDCl_3$, 25 °C): δ [ppm] = 8.32 (s, 2H, H-3), 8.17-8.15 (m, 2H, H-16), 7.91-7.88 (m, 2H, H-13), 7.83 (dd, $^{3}J_{HH}$ = 6.6 Hz, $^{4}J_{HH}$ = 2.7 Hz, 2H, H-12), 7.73 (d, $^{3}J_{HH}$ = 8.4 Hz, 2H, H-6), 7.53-7.50 (m, 4H, H-14, H-15), 7.45-7.42 (m, 4H, H-10, H-11), 7.39 (d, $^{3}J_{HH}$ = 8.6 Hz, 2H, H-22), 6.59 (d, $^{3}J_{HH}$ = 8.8 Hz, 2H, 23), 6.04 (quint, $^{3}J_{HH}$ = 7.5 Hz, 2H, H-7), 3.29 (t, $^{3}J_{HH}$ = 7.7 Hz, 4H, H-25), 1.65 (d, $^{3}J_{HH}$ = 6.8 Hz, 6H, H-8), 1.63-1.56 (m, 4H, H-26), 1.36-1.30 (m, 12H, H-27, H-28, H-29), 0.93-0.89 (m, 6H, H-30).

^{13}C-NMR (100 MHz, $CDCl_3$, 25 °C): δ [ppm] = 162. 5 (C-5), 149.1 (C-24), 148.8 (C-2), 138.3 (C-9), 136.2 (C-4), 134.2 (C-18), 134.0 (C-22), 131.2 (C-17), 129.1 (C-13), 128.6 (C-12), 126.8 (C-14), 126.4 (C-3), 126.1 (C-15), 125.4 (C-11), 123.5 (C-16), 122.9 (C-10), 111.3 (C-23), 106.8 (C-21), 99.9 (C-20), 85.2 (C-19), 51.1 (C-25), 45.4 (C-7), 31.8 (C-28), 27.3 (C-26), 26.9 (C-27), 22.8 (C-29), 21.2 (C-8), 14.2 (C-30).

HRMS (ESI): found 757.4457 m/z $[M+H]^+$, calculated for $C_{51}H_{57}N_4O_2$ 757.4476 m/z.

(*S,S*)-L^{NHex2}: 72% yield

^{1}H-NMR (400 MHz, $CDCl_3$, 25 °C): δ [ppm] = 8.32 (s, 2H, H-3), 8.18-8.15 (m, 2H, H-16), 7.91-7.87 (m, 2H, H-13), 7.83 (dd, $^{3}J_{HH}$ = 6.6 Hz, $^{4}J_{HH}$ = 2.8 Hz, 2H, H-12), 7.74 (d, $^{3}J_{HH}$ = 8.4 Hz, 2H, H-6), 7.54-7.49 (m, 4H, H-14, H-15), 7.44-7.42 (m, 4H, H-10, H-11), 7.39 (d, $^{3}J_{HH}$ = 8.7 Hz, 2H, H-22), 6.59 (d, $^{3}J_{HH}$ = 8.8 Hz, 2H, 23), 6.03 (quint, $^{3}J_{HH}$ = 7.3 Hz, 2H, H-7), 3.29 (t, $^{3}J_{HH}$ = 7.7 Hz, 4H, H-25), 1.65 (d, $^{3}J_{HH}$ = 6.7 Hz, 6H, H-8), 1.63-1.56 (m, 4H, H-26), 1.36-1.30 (m, 12H, H-27, H-28, H-29), 0.94-0.88 (m, 6H, H-30).

^{13}C-NMR (100 MHz, $CDCl_3$, 25 °C): δ [ppm] = 162. 5 (C-5), 149.1 (C-24), 148.8 (C-2), 138.3 (C-9), 136.2 (C-4), 134.2 (C-18), 133.9 (C-22), 131.1 (C-17), 129.1 (C-13), 128.6 (C-12), 126.8 (C-14), 126.4 (C-3), 126.1 (C-15), 125.4 (C-11), 123.5 (C-16), 122.9 (C-10), 111.3 (C-23), 106.8 (C-21), 99.9 (C-20), 85.2 (C-19), 51.1 (C-25), 45.4 (C-7), 31.8 (C-28), 27.3 (C-26), 26.9 (C-27), 22.8 (C-29), 21.1 (C-8), 14.2 (C-30).

HRMS (ESI): found 757.4463 m/z $[M+H]^+$, calculated for $C_{51}H_{57}N_4O_2$ 757.4476 m/z.

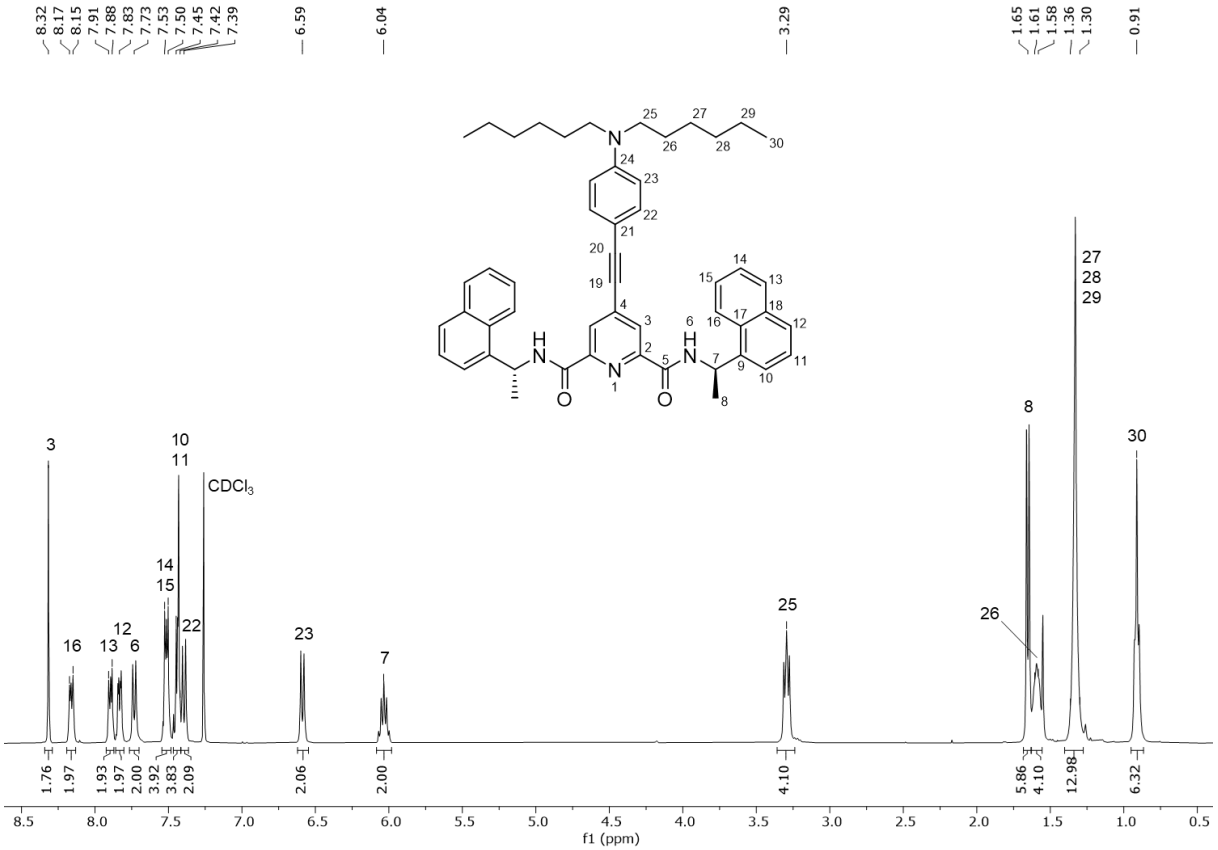

Figure S3: *^{1}H-NMR spectrum (400 MHz, $CDCl_3$, 25 °C) of ligand* ***(R,R)-L^{NHex2}*** *with assigned signals.*

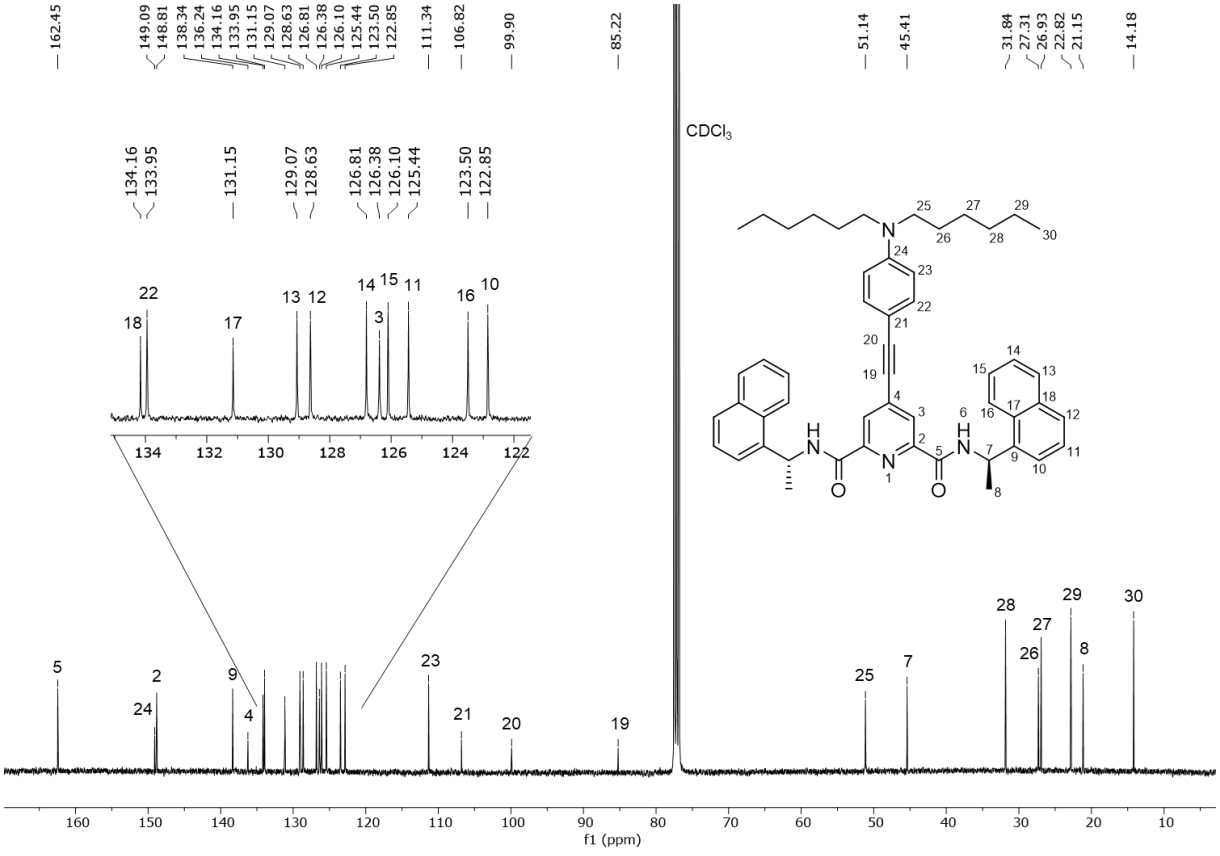

Figure S4: *^{13}C-NMR spectrum (100 MHz, $CDCl_3$, 25 °C) of ligand* ***(R,R)-L^{NHex2}*** *with assigned signals.*

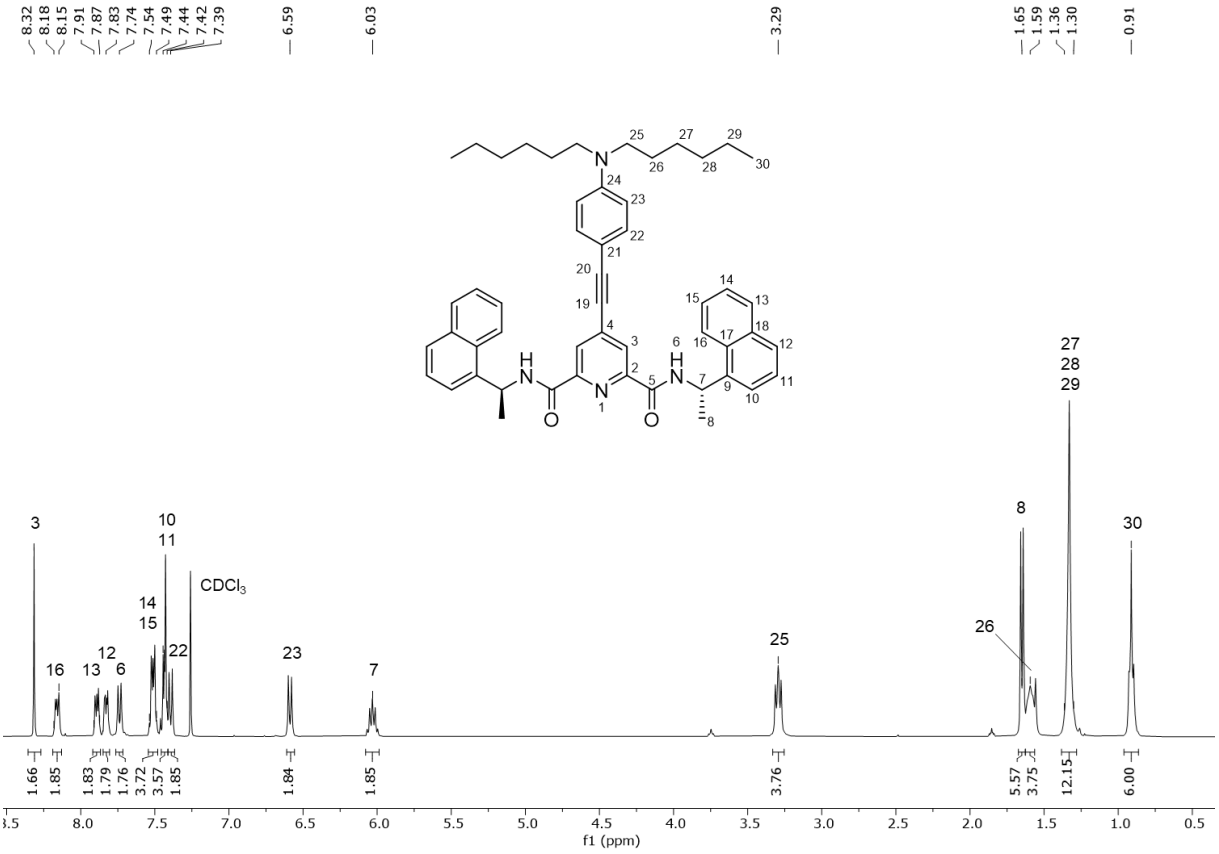

Figure S5: *^{1}H-NMR spectrum (400 MHz, $CDCl_3$, 25 °C) of ligand* ***(S,S)-L^{NHex2}*** *with assigned signals.*

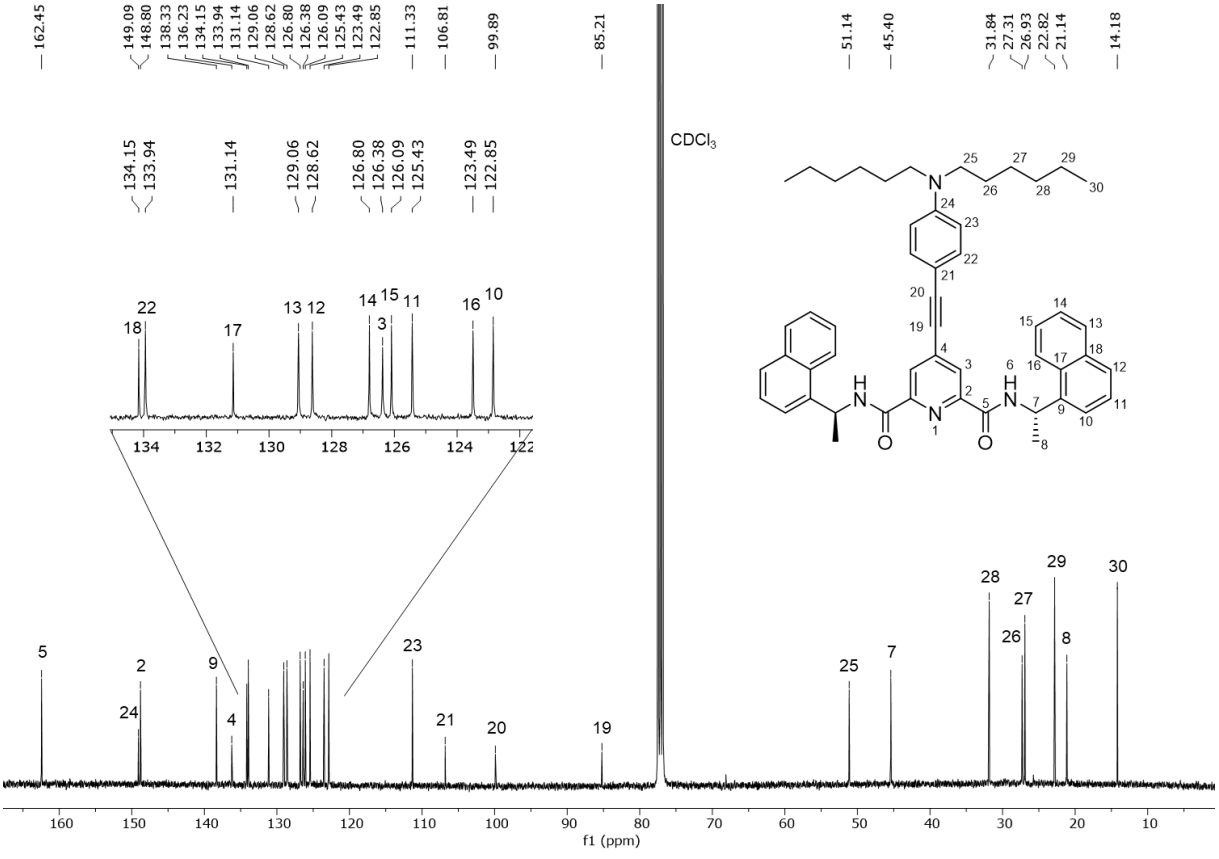

Figure S6: *^{13}C-NMR spectrum (100 MHz, $CDCl_3$, 25 °C) of ligand* ***(S,S)-L^{NHex2}*** *with assigned signals.*

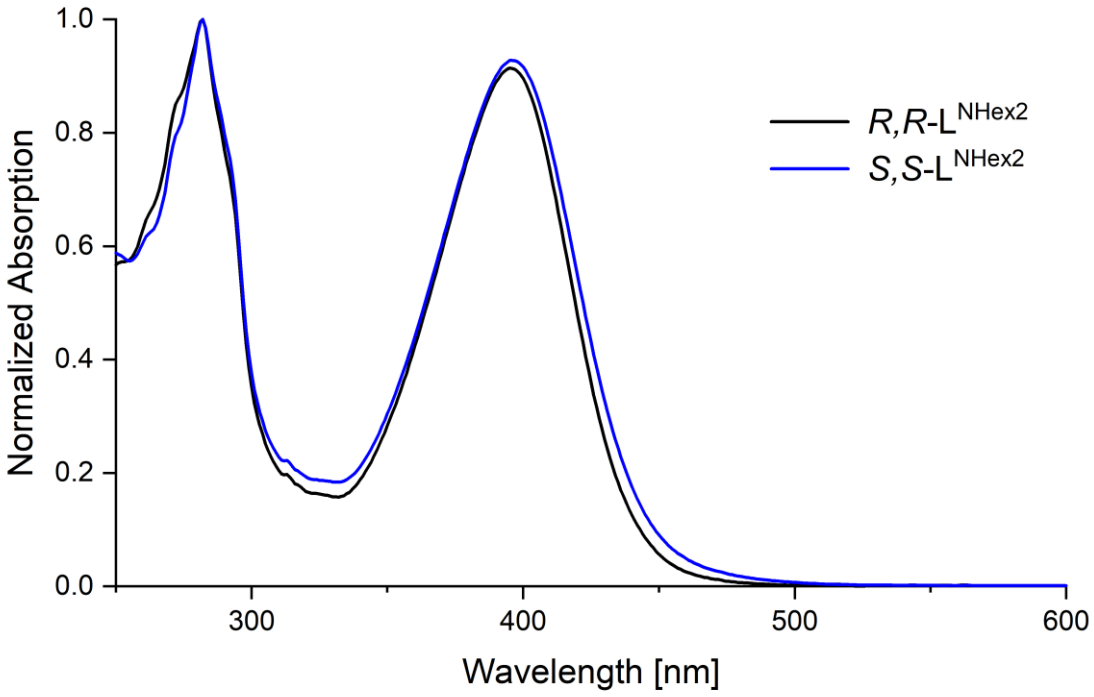

Figure S7: *Absorption spectra of the ligands R,R-L^{NHex2} (black line) and R,R-L^{NHex2} (blue line) in methanol at 298 K.*

S 4. COMPLEX SYNTHESES

GENERAL PROCEDURE

The ligand of interest was dissolved in 40 mL of a 1:1 mixture of methanol and dichloromethane under argon atmosphere. The respective lanthanide triflate salt was added and the solution was stirred overnight at 40 °C, followed by additional 2 h at 50 °C. After solvent removal under reduced pressure, the crude product was purified by washing with diethyl ether, centrifugation (4000 rpm, 10 min) and decantation of the supernatant solution. This procedure was repeated three times and the complex was dried under vacuum prior to further analysis.

[Yb(*R,R*-L^{NHex2})$_3$(OTf)$_3$] / Δ-Yb

The complex was synthesized according to the general procedure, using **(*R,R*)-L^{NHex2}** (3 equiv.) and Yb(OTf)$_3$ (1 equiv.) to yield the desired complex as an orange powder.

^{1}H-NMR (300 MHz, CD$_3$OD, 25 °C): δ [ppm] = 15.51 (br, 2H, H-7), 13.35 (d, $^3J_{HH}$ = 6.0 Hz 2H, H-16), 9.28 (t, $^3J_{HH}$ = 7.1 Hz, 2H, H-15), 7.33 (t, $^3J_{HH}$ = 8.0 Hz, 2H, H-14), 6.73 (d, $^3J_{HH}$ = 9.0 Hz, 2H, H-22), 6.53 (d, $^3J_{HH}$ = 8.0 Hz, H-13), 6.42 (d, $^3J_{HH}$ = 8.8 Hz, 2H, H-23), 5.39 (d, $^3J_{HH}$ = 8.4 Hz, 2H, H-12), 4.21 (t, $^3J_{HH}$ = 6.8 Hz, 2H, H-11), 3.40 (br, 6H, H-8), 3.20 (t, $^3J_{HH}$ = 7.2 Hz, 4H, H-25), 2.50 (s, 2H, H-3), 2.03

(br, 2H, H-10), 1.48-1.37 (m, 4H, H-26), 1.28-1.16 (m, 12H, H-27, H-28, H-29), 0.81 (t, $^3J_{HH}$ = 6.6 Hz, 6H, H-30).

HRMS (ESI): Found 611.0681 m/z [2L, 1L+H$^+$, Yb^{3+}]$^{4+}$, calculated for $C_{153}H_{169}N_{12}O_6Yb^{4+}$ 611.0671 m/z. Found 1221.1266 m/z [2L, 1L-H$^-$, Yb^{3+}]$^{2+}$, calculated for $C_{153}H_{167}N_{12}O_6Yb^{2+}$ 1221.1269 m/z. Found 1296.1062 m/z [3L, Yb^{3+}, OTf$^-$]$^{2+}$, calculated for $C_{154}H_{168}F_3N_{12}O_9SYb^{2+}$ 1296.6077 m/z.

[Yb(*S,S*-L^{NHex2})$_3$(OTf)$_3$] / Λ-Yb

The complex was synthesized according to the general procedure, using **(*S,S*)-L^{NHex2}** (3 equiv.) and Yb(OTf)$_3$ (1 equiv.) to yield the desired complex as an orange powder.

^{1}H-NMR (300 MHz, CD$_3$OD, 25 °C): δ [ppm] = 15.42 (br, 2H, H-7), 13.29 (br, 2H, H-16), 9.26 (br, 2H, H-15), 7.34 (t, $^3J_{HH}$ = 7.4 Hz, 2H, H-14), 6.74 (d, $^3J_{HH}$ = 9.0 Hz, 2H, H-22), 6.54 (d, $^3J_{HH}$ = 8.1 Hz, H-13), 6.42 (d, $^3J_{HH}$ = 9.0 Hz, 2H, H-23), 5.42 (d, $^3J_{HH}$ = 8.1 Hz, 2H, H-12), 4.23 (br, 2H, H-11), 3.38 (br, 6H, H-8), 3.20 (t, $^3J_{HH}$ = 7.5 Hz, 4H, H-25), 2.54 (s, 2H, H-3), 2.08 (br, 2H, H-10), 1.47-1.39 (m, 4H, H-26), 1.28-1.16 (m, 12H, H-27, H-28, H-29), 0.81 (t, $^3J_{HH}$ = 6.6 Hz, 6H, H-30).

HRMS (ESI): Found 814.4210 m/z [3L, Yb^{3+}]$^{3+}$, calculated for $C_{153}H_{168}N_{12}O_6Yb^{3+}$ 814.4203 m/z. Found 1221.1270 m/z [2L, 1L-H$^-$, Yb^{3+}]$^{2+}$, calculated for $C_{153}H_{167}N_{12}O_6Yb^{2+}$ 1221.1269 m/z.

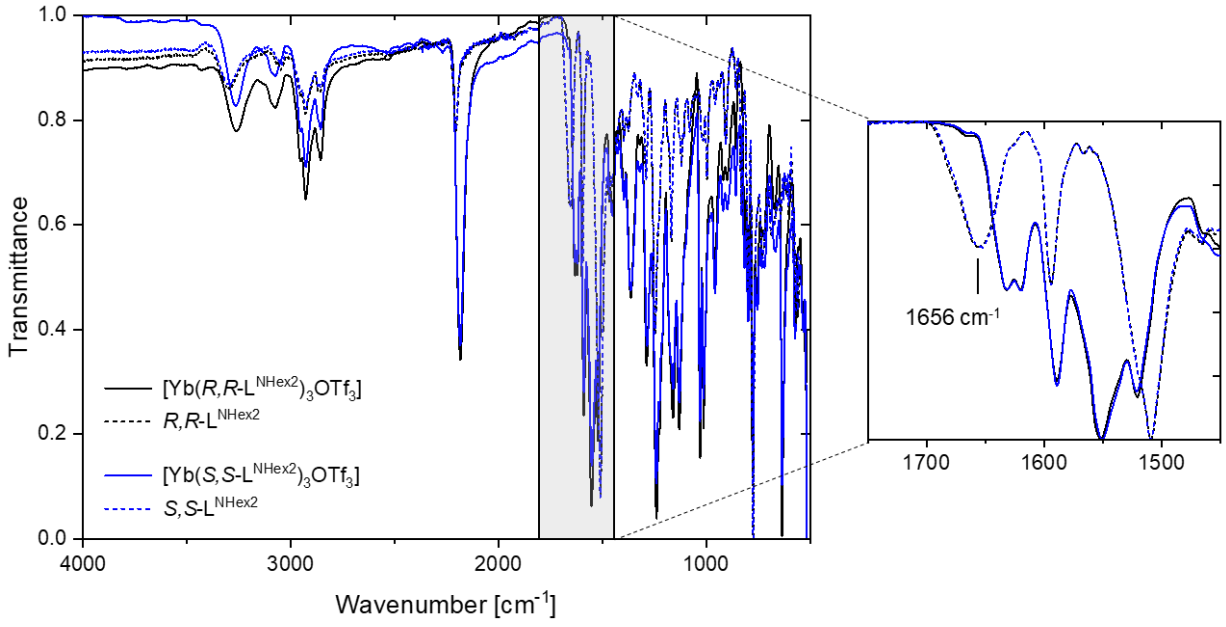

Figure S8: *FTIR spectra of the two Yb(III) complexes (solid lines) and the corresponding ligands (dashes lines) with enlarged region of the ligands' carbonyl vibration.*

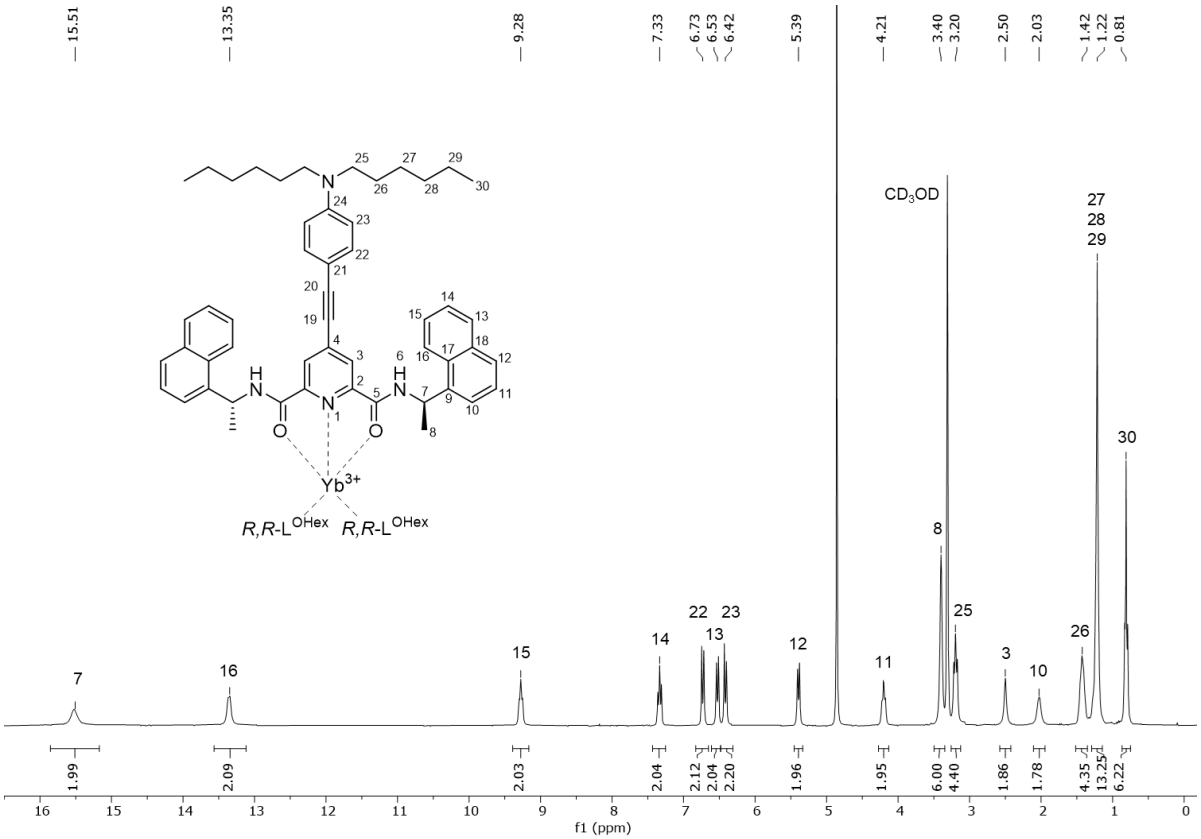

Figure S9: *^{1}H-NMR spectrum (300 MHz, CD_3OD, 25 °C) of complex [Yb(R,R-L^{NHex2})$_3$(OTf)$_3$]. Signals are assigned in accordance with designation of ligand protons.*

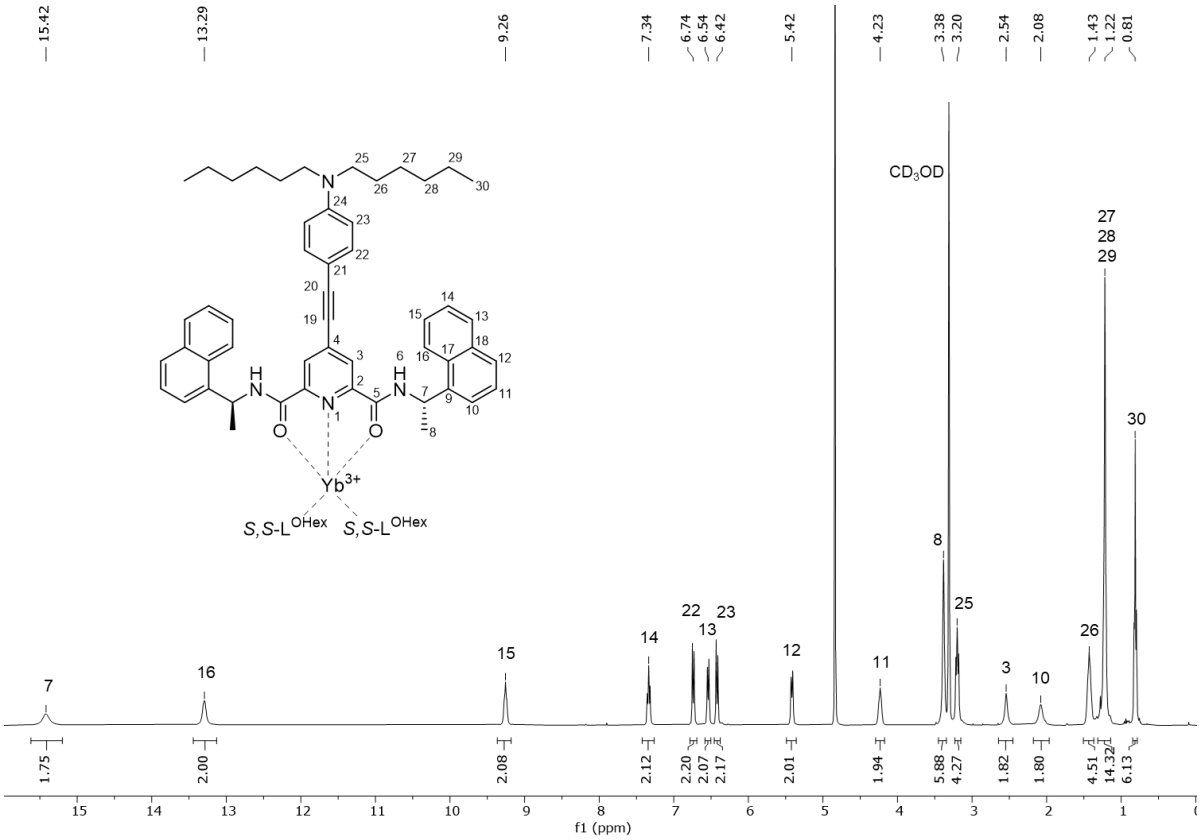

Figure S10: *^{1}H-NMR spectrum (300 MHz, CD_3OD, 25 °C) of complex [Yb(S,S-L^{NHex2})$_3$(OTf)$_3$]* ***Δ-Yb****. Signals are assigned in accordance with designation of ligand protons.*

S 5. CRYSTAL STRUCTURE

***Table S1**. Summary of X-ray crystallographic data for [Yb(S,S-L^{NHex2})$_3$(OTf)$_3$] / **Δ-Yb** and [Yb(R,R-L^{NHex2})$_3$(OTf)$_3$] / **Λ-Yb**.*

Compound	{[Yb(*S,S*-L^{NHex2})$_3$](OTf)$_3$} **Δ-Yb**	{[Yb(*R,R*-L^{NHex2})$_3$](OTf)$_3$} **Λ-Yb**
Formula	$C_{156}H_{168}F_9N_{12}O_{15}S_3Yb$	$C_{156}H_{168}F_9N_{12}O_{15}S_3Yb$
M / g.mol^{-1}	2891.23	2891.23
Crystal system	orthorhombic	Orthorhombic
Space group	$P2_12_12_1$ (N°19)	$P2_12_12_1$ (N°19)
Cell parameters	a = 22.207(4) Å b = 26.800(5) Å c = 31.519(5) Å	a = 22.181(4)Å b = 26.777(6)Å c = 31.548(7) Å
Volume / Å^3	18758(6)	18738(7)
Z	4	4
T / K	150 K	150 K
2θ range /°	3.514 ≤ 2θ ≤ 55.262	4.16 ≤ 2θ ≤ 55.042
ρ_{calc} / g.cm^{-3}	1.024	1.025
μ / mm^{-1}	0.592	0.593
Number of reflections	147447	248713
Independent reflections	43138	42947
R_{int}	0.1194	0.0776
$Fo^2 > 2\sigma(Fo)^2$	22418	31840
Number of variables	1753	1760
R_1, ωR_2 Flack parameter	0.0755, 0.1806 0.020(12)	0.0485, 0.1167 -0.008(3)
CCDC number	2245303	2245302

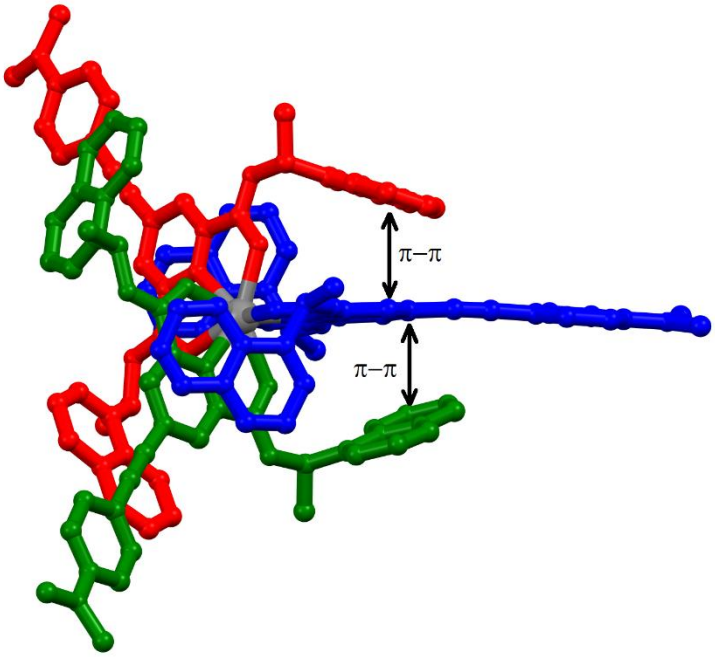

***Figure S11**: Molecular structure of [Yb(R,R-L^{NHex2})$_3$(OTf)$_3$] / **Λ-Yb**. The three R,R-L^{NHex2} ligands are drawn in blue, green and red and the intramolecular π-π interactions are highlighted.*

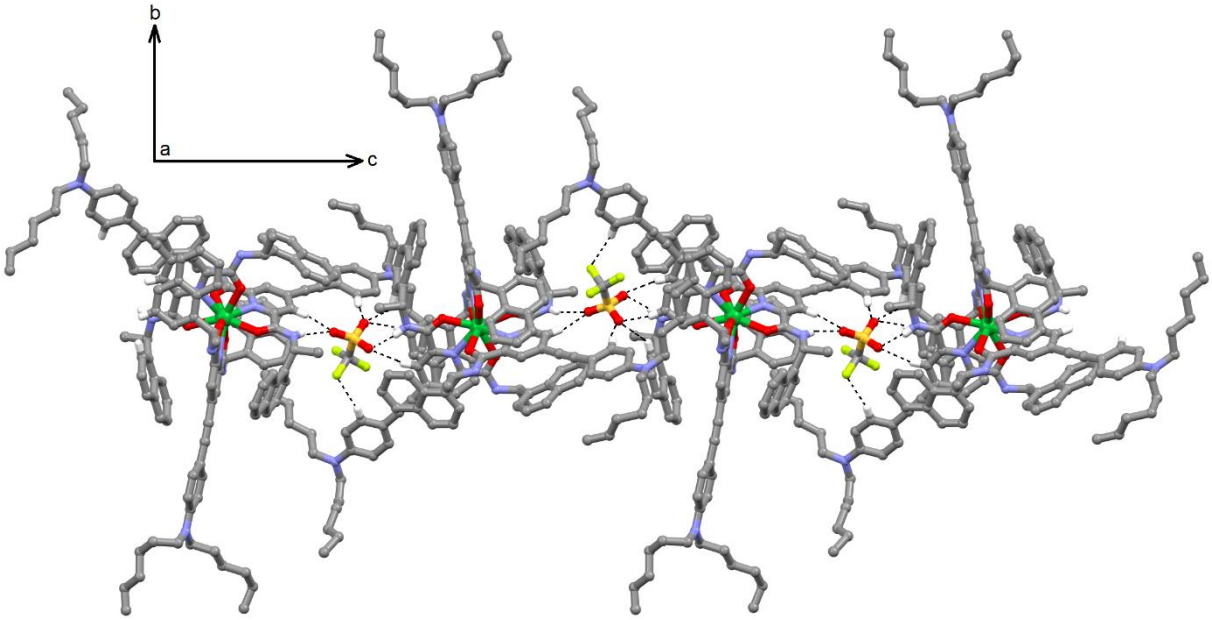

***Figure S12**: Crystal packing view of [Yb(R,R-L^{NHex2})$_3$(OTf)$_3$] **Λ-Yb** in the (011) plan highlighting the template effect of the OTf$^-$ anion through hydrogen bond, H-F and H-O contacts (dashed black lines).*

S 6. PREPARATION OF THE PDMS SAMPLES

For the preparation of poly(dimethylsiloxane) (PDMS) specimens, we used the two-component (pre-polymer and cross-linker) Sylgard 184 polymerization kit commercially available from Dow. For all samples a concentration of 0.5 mg of the complex per 1 g poly(dimethylsiloxane) was used. A solution of the desired complex (0.5 mg) in THF (0.25 mL) was added to the PDMS base component (1 g) and mixture was manually homogenized using a spatula and evacuated for at least 15 min under a vacuum bell to avoid the inclusion or air bubbles. The PDMS crosslinking component was added and after further homogenization the mixture was evacuated for further 15 min, before it was molded into the Cu-support, the EPR tube or the container of choice by a 1 mL syringe. The resin was cured at room temperature under vacuum for 48 h. For variable-temperature CPL measurements the sample holder (Figure S13 b) contained samples of the complex, immobilized in PDMS, as well as a blank, pristine polymer.

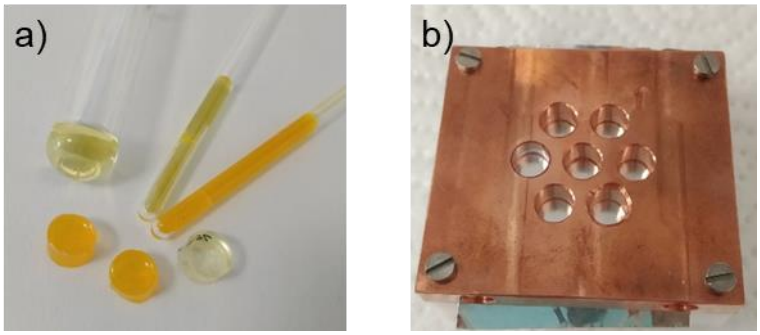

Figure S13. *(a) PDMS samples containing the complexes [Yb(R,R-L^{NHex2})$_3$(OTf)$_3$] and [Yb(S,S-L^{NHex2})$_3$(OTf)$_3$] in different concentrations. (b) Copper-based support used for temperature-dependent NIR-CPL measurements.*

S 7. PHOTOPHYSICAL COMPLEX CHARACTERIZATION

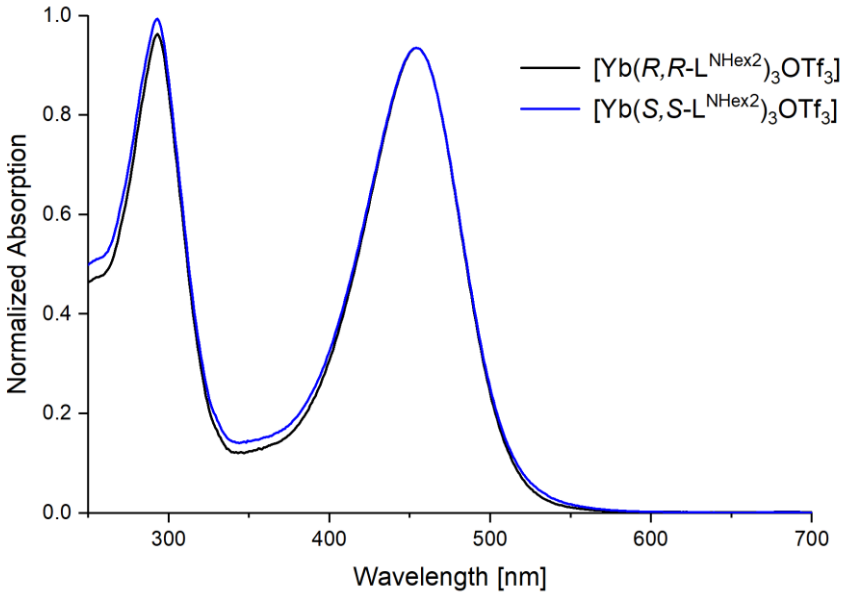

Figure S14. *UV/vis region absorption spectra of the complexes [Yb(R,R-L^{NHex2})$_3$(OTf)$_3$] and [Yb(S,S-L^{NHex2})$_3$(OTf)$_3$] in methanol at 298 K.*

Table S2: *Extinction coefficients of the complexes [Yb(R,R-L^{NHex2})$_3$(OTf)$_3$] and [Yb(S,S-L^{NHex2})$_3$(OTf)$_3$] calculated from optical densities of complex solutions in methanol at 292 nm and 454 nm.*

	[Yb(*R*,*R*-L^{NHex2})$_3$(OTf)$_3$]	**[Yb(*S*,*S*-L^{NHex2})$_3$(OTf)$_3$]**
ε [L/mol*cm] at λ = 292 nm	96000	106000
ε [L/mol*cm] at λ = 454 nm	83000	83000

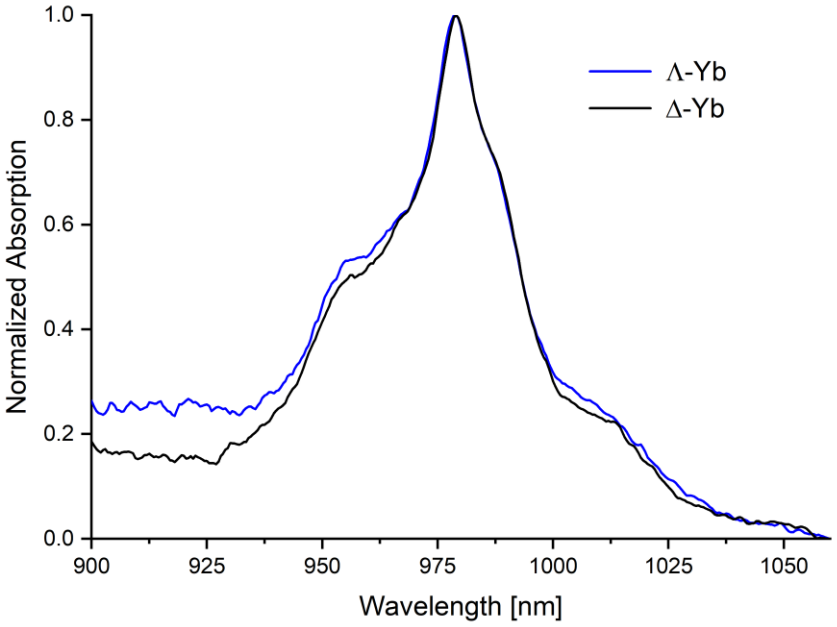

Figure S15. *NIR region absorption spectra of complexes [Yb(R,R-L^{NHex2})$_3$(OTf)$_3$] / **Λ-Yb** (blue line) and [Yb(S,S-L^{NHex2})$_3$(OTf)$_3$] / **Δ-Yb** (black line) in methanol at 298 K (c ≈ 8*10^{-4} M).*

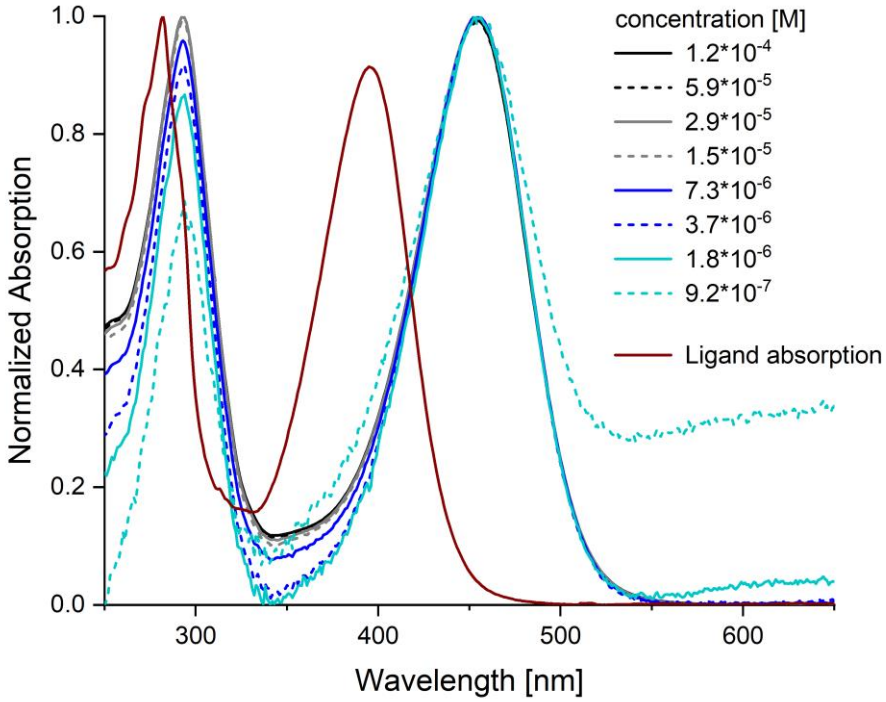

Figure S16. *Absorption spectra of the complex [Yb(R,R-L^{NHex2})$_3$(OTf)$_3$] dissolved in methanol at various concentration with absorption spectrum of the respective ligand R,R-L^{NHex2}.*

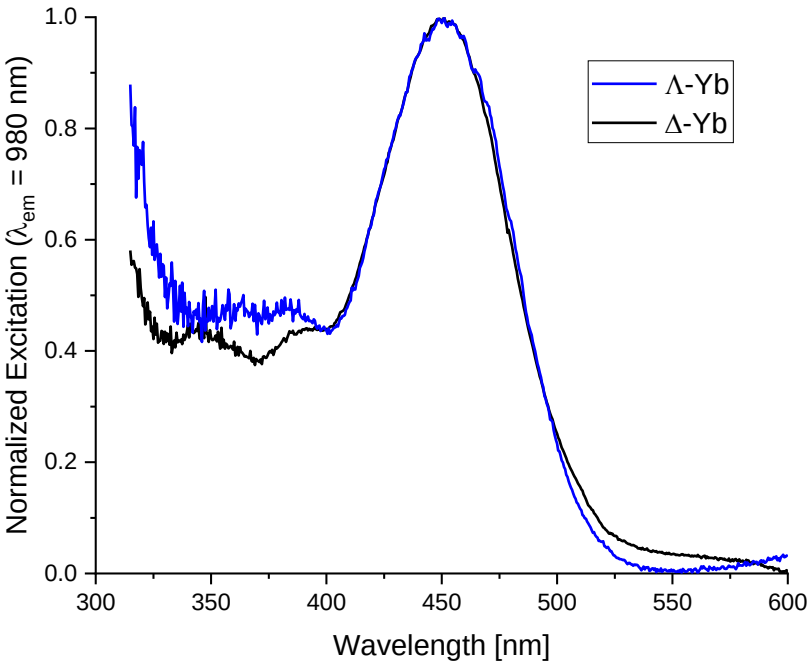

Figure S17. *Excitation spectra of the complex [Yb(R,R-L^{NHex2})$_3$(OTf)$_3$] dissolved in methanol (λ_{em}=980 nm).*

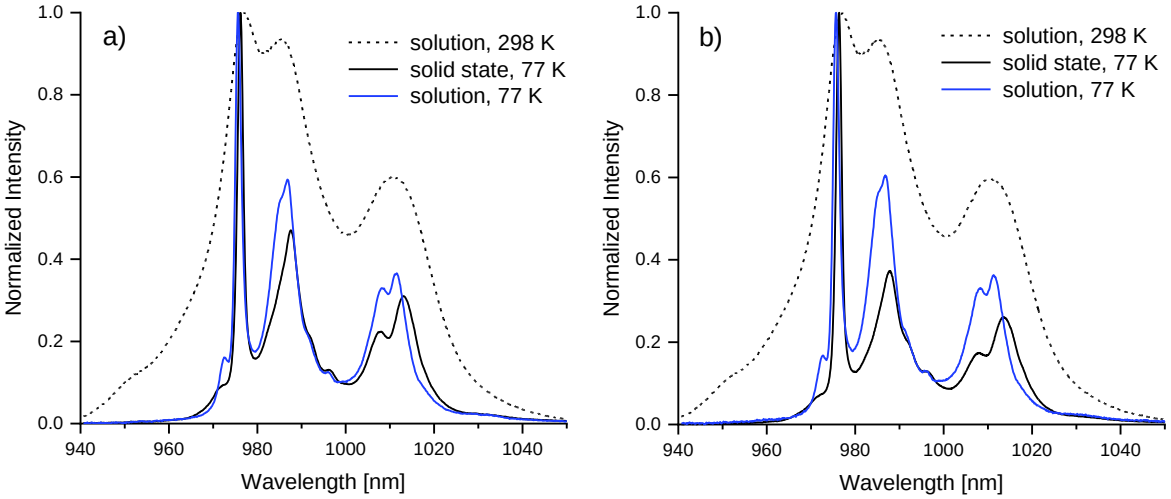

Figure S18. *Luminescence spectra of the two enantiomers (a) [Yb(R,R-L^{NHex2})$_3$(OTf)$_3$] and (b) [Yb(S,S-L^{NHex2})$_3$(OTf)$_3$] in solution of a 4:1 ethanol/methanol mixture at 298 K and at 77 K and in solid state at 77 K (λ_{ex} = 350 nm).*

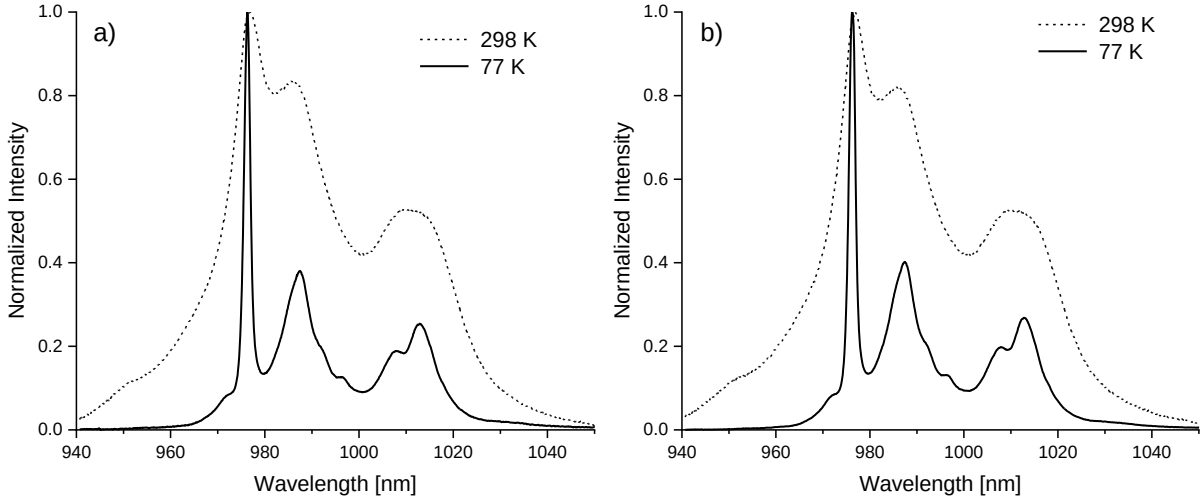

Figure S19. *Luminescence spectra of the two enantiomers (a) [Yb(R,R-L^{NHex2})$_3$(OTf)$_3$] and (b) [Yb(S,S-L^{NHex2})$_3$(OTf)$_3$] in PDMS matrix at 298 K and at 77 K (λ_{ex}=350 nm).*

Table S3: *Luminescence lifetimes at 980 nm determined for the complexes [Yb(R,R-L^{NHex2})$_3$(OTf)$_3$] and [Yb(S,S-L^{NHex2})$_3$(OTf)$_3$] from their luminescence decay recorded at 298 K.*

	Luminescence lifetime [10^{-6} s]	
medium	**[Yb(*R*,*R*-L^{NHex2})$_3$OTf$_3$]**	**[Yb(*S*,*S*-L^{NHex2})$_3$OTf$_3$]**
powder	5.25	4.55
methanol	5.91	5.90
PDMS	4.84	4.91

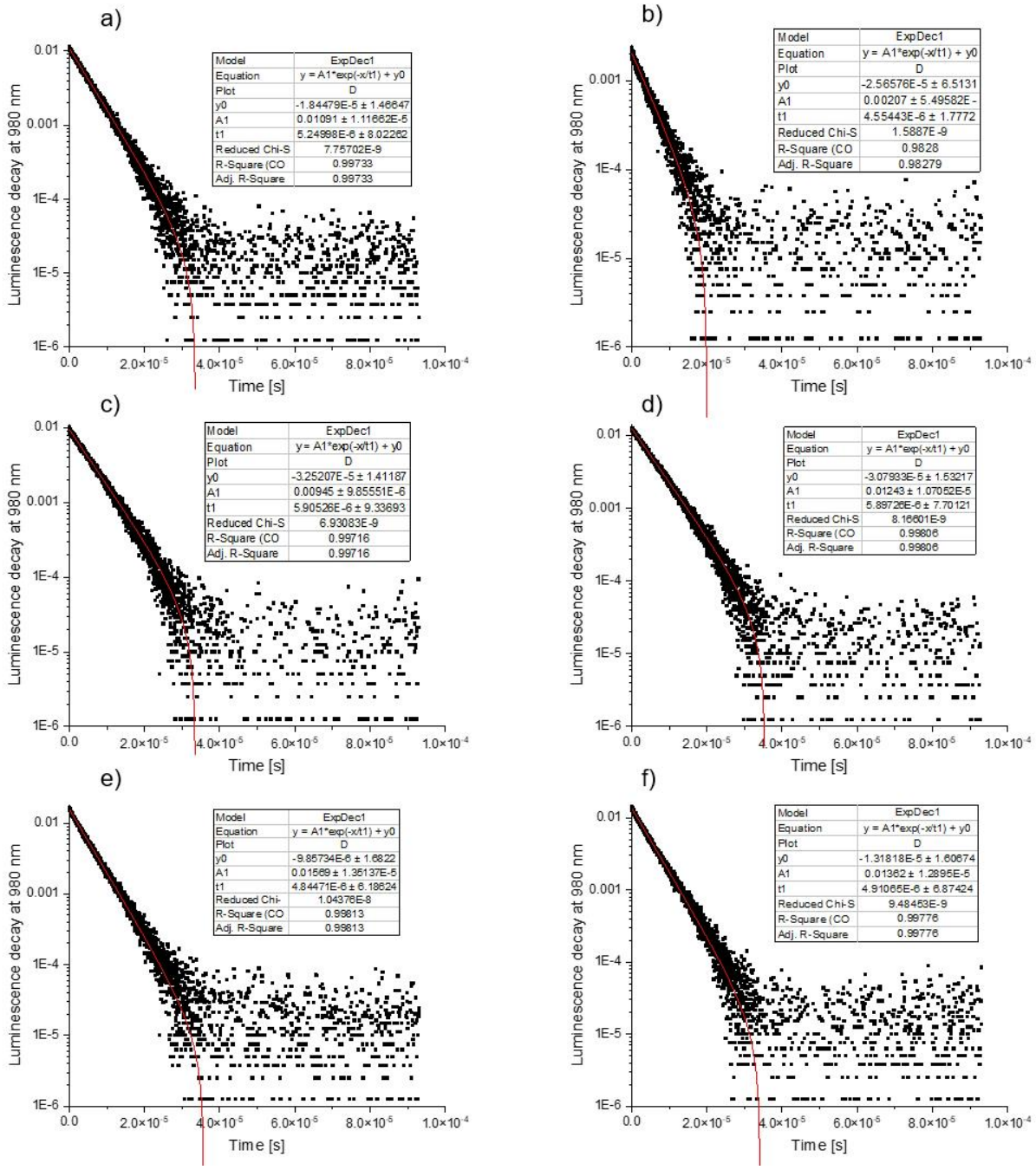

Figure S20. *Luminescence decays at 980 nm (black) and monoexponential fits (red) recorded for the complexes [Yb(R,R-L^{NHex2})$_3$(OTf)$_3$] (a, c, e) and [Yb(S,S-L^{NHex2})$_3$(OTf)$_3$] (b, d, f) determined as powder (a, b), in methanol solution (c, d) and immobilized in PDMS matrix (e, f) at 298 K (λ_{ex} = 400 nm).*

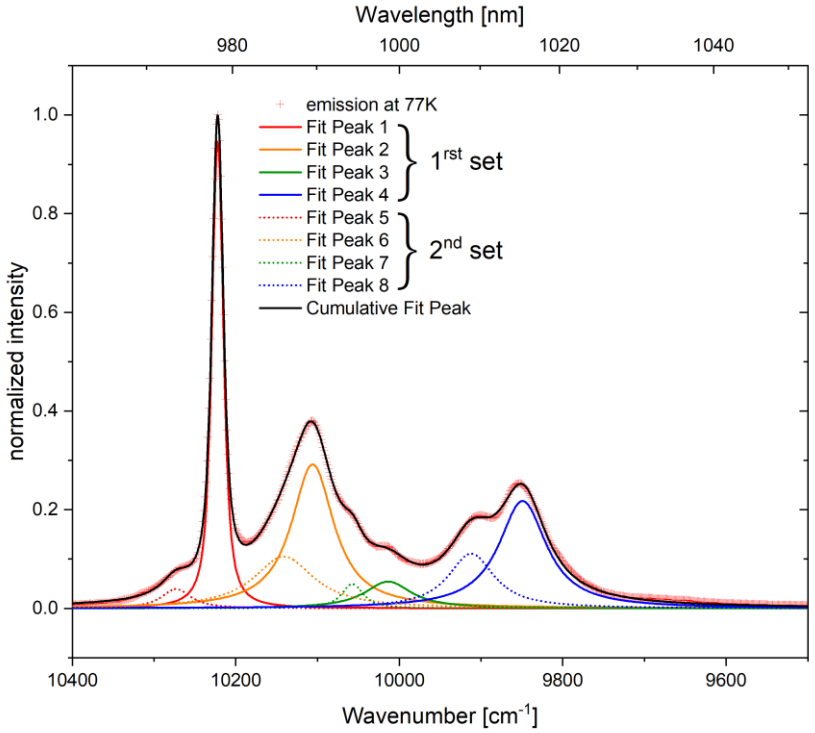

Plot	1	2	3	4	5	6	7	8
position	10222.23 ± 0.01	10106.03 ± 0.54	10013.64 ± 1.27	9849.17 ± 0.26	10272.96 ± 0.64	10141.35 ± 3.46	10057.32 ± 0.60	9912.05 ± 0.48
area	22.02 ± 0.12	28.47 ± 2.53	5.87 ± 0.48	23.99 ± 0.46	2.63 ± 0.13	14.694 ± 2.62	2.37 ± 0.40	11.754 ± 0.50
gaussian width	9.62 ± 0.18	9.62 ± 0.18	9.62 ± 0.18	9.62 ± 0.18	9.62 ± 0.18	9.62 ± 0.18	9.62 ± 0.18	9.62 ± 0.18
lorentzian width	11.04 ± 0.18	61.05 ± 2.34	67.90 ± 4.52	69.234 ± 1.08	41.15 ± 2.20	88.08 ± 4.53	28.48 ± 3.50	66.36 ± 2.07
Reduced Chi-Sqr	1.40849E-5							
R-Square (COD)	0.99937							
Adj. R-Square	0.99935							

Figure S21. *Voigt decomposition of the luminescence spectrum of [Yb(R,R-L^{NHex2})$_3$(OTf)$_3$] in PDMS matrix at 77 K (spectral bandwidth: 1 nm, λ_{ex}= 350 nm).*

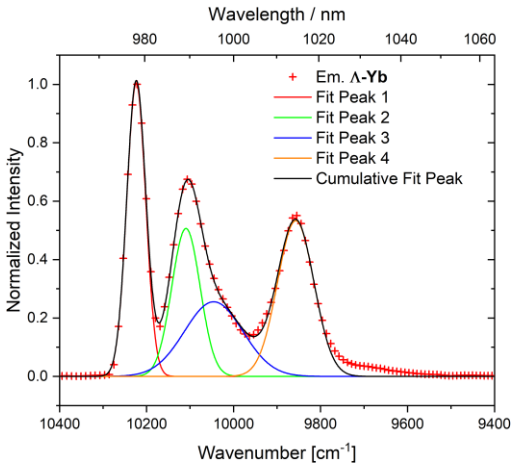

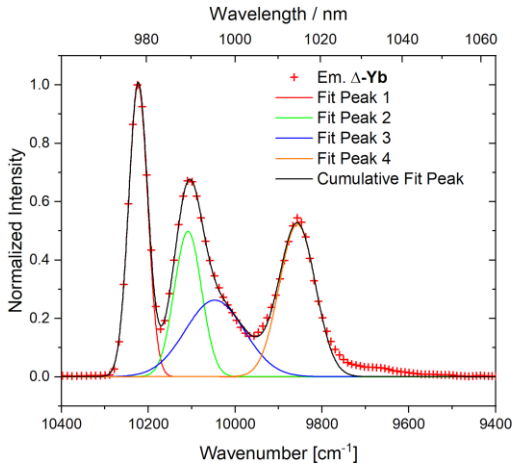

Plot	Peak 1	Peak 2	Peak 3	Peak 4
Position	10223.74607 ± 0.27286	10109.419 ± 0.79974	10045.73127 ± 14.72676	9857.10017 ± 0.58133
Width	43.52527 ± 0.54009	65.27553 ± 4.08608	133.99451 ± 15.96366	83.62535 ± 1.408
Area	54.79277 ± 1.08603	41.4343 ± 7.84544	42.89818 ± 9.26092	55.86589 ± 0.9197
Reduced Chi-Sqr	9.95093E-5			
R-Square (COD)	0.99874			
Adj. R-Square	0.99845			

Plot	Peak 1	Peak 2	Peak 3	Peak 4
Position	10223.28104 ± 0.19877	10108.66437 ± 0.58632	10046.82671 ± 8.25237	9856.76495 ± 0.42738
Width	43.69277 ± 0.39997	62.57643 ± 2.52325	135.94719 ± 8.98437	83.12538 ± 1.08132
Area	54.70232 ± 0.75815	39.07078 ± 4.35279	44.70736 ± 5.27003	54.41756 ± 0.66315
Reduced Chi-Sqr	5.63544E-5			
R-Square (COD)	0.99918			
Adj. R-Square	0.99907			

Figure S22. *Gaussian decomposition of the luminescence spectra of Λ-Yb (on the left) and Δ-Yb (on the right) in PDMS matrix at 4 K (spectral bandwidth: 4 nm, λ_{ex} = 365 nm).*

S 8. CHIROPTICAL MEASUREMENTS

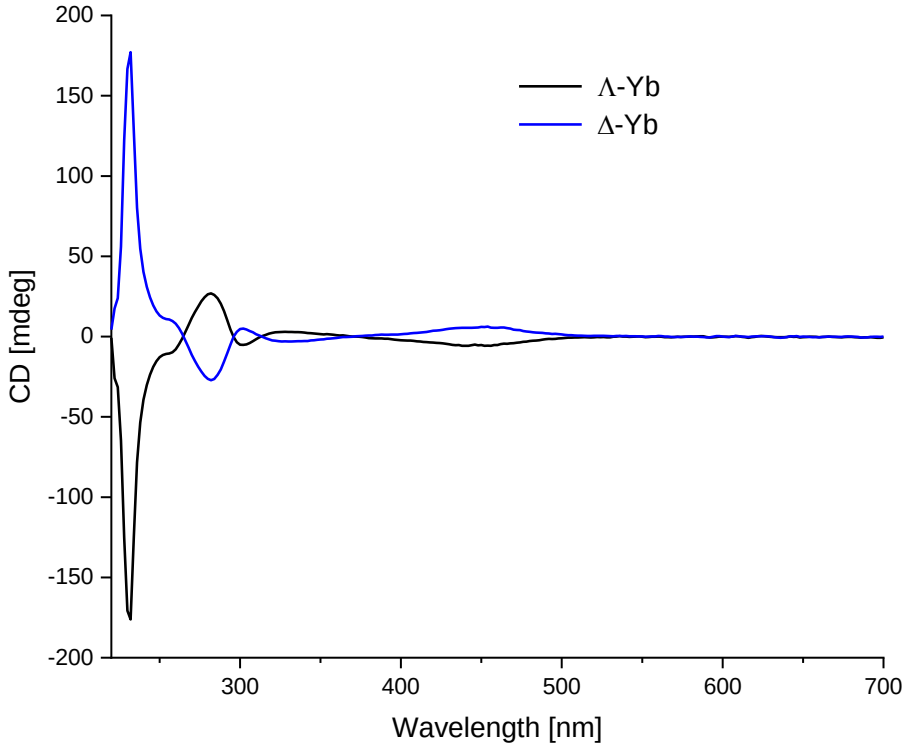

Figure S23. *Circular dichroism spectra of the complexes [Yb(R,R-L^{NHex2})$_3$(OTf)$_3$] /* ***Λ-Yb*** *(black line) and [Yb(S,S-L^{NHex2})$_3$(OTf)$_3$] /* ***Δ-Yb*** *(blue line) in methanol at 298 K.*

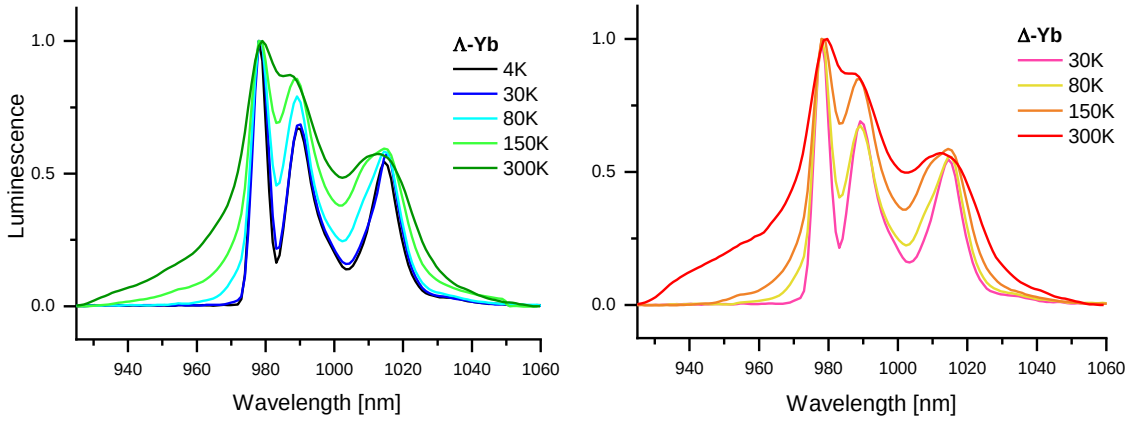

Figure S24. *Luminescence spectra of [Yb(R,R-L^{NHex2})$_3$(OTf)$_3$] /* **Λ-Yb** *(a) and [Yb(S,S-L^{NHex2})$_3$(OTf)$_3$] /* **Δ-Yb** *(b), immobilized in PDMS matrix (λ_{ex} = 365 nm), recorded at variable temperature in parallel to the corresponding CPL measurements (cf. Figure 5).*

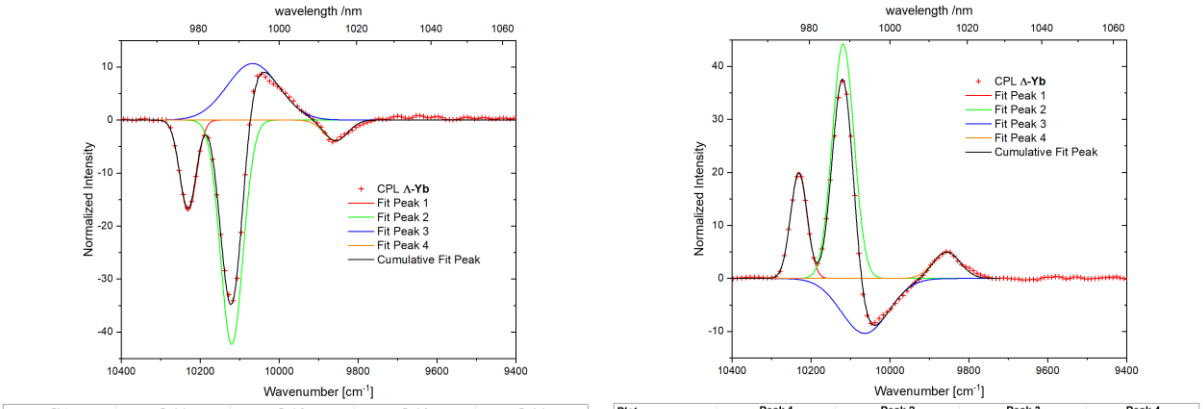

Plot	Peak 1	Peak 2	Peak 3	Peak 4
Position	10230.55787 ± 0.79524	10120.15512 ± 0.43096	10066.78085 ± 11.01137	9856.46357 ± 2.73192
Width	42.25026 ± 1.61015	56.9615 ± 1.72893	129.59373 ± 10.02966	60.7769 ± 5.89946
Area	-907.3934 ± 48.44067	-3019.92942 ± 229.74391	1731.97356 ± 277.84223	-301.04647 ± 24.65849
Reduced Chi-Sqr	0.31327			
R-Square (COD)	0.99747			
Adj. R-Square	0.99688			

Plot	Peak 1	Peak 2	Peak 3	Peak 4
Position	10230.38957 ± 0.36844	10118.3972 ± 0.21261	10063.44393 ± 6.53811	9856.39392 ± 1.45402
Width	41.79771 ± 0.72984	54.94174 ± 0.96129	119.01007 ± 6.1896	69.38281 ± 3.33717
Area	1050.76245 ± 21.52813	3045.85202 ± 137.42992	-1543.91398 ± 158.46548	432.93332 ± 16.95892
Reduced Chi-Sqr	0.11334			
R-Square (COD)	0.99862			
Adj. R-Square	0.99844			

Figure S25. *Gaussian decomposition of the CPL spectra of Λ-Yb (on the left) and Δ-Yb (on the right) in PDMS matrix at 4 K (spectral bandwidth: 4 nm, λ_{ex} = 365 nm).*

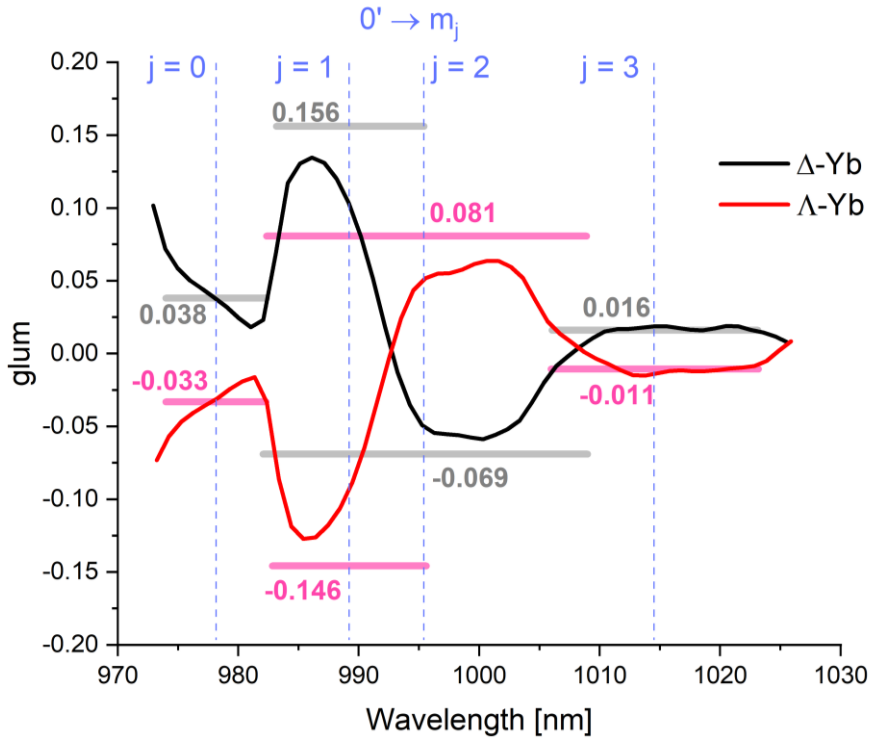

Figure S26. *Variations of the emission dissymmetry factor, g_{lum}, of **Λ-Yb** and **Δ-Yb** over the emission range (cut-off at 5% of the emission maximum) at 4K (spectral bandwidth: 4 nm). The horizontal bars represent the g_{lum} extracted by comparing areas of the gaussian decomposition of CPL and luminescence, with a width corresponding to twice the FWHM of each contribution.*

Table S4: *g_{lum} dissymmetry factors calculated from CPL spectra at variable temperature, as depicted in Figure S25. As respective wavelengths, the four arbitrary wavelengths were chosen to exemplarily illustrate the change of g_{lum} with increasing temperature.*

T [K]	986 nm		994 nm		1002 nm		1015 nm	
	Δ-Yb	**Λ-Yb**	**Δ-Yb**	**Λ-Yb**	**Δ-Yb**	**Λ-Yb**	**Δ-Yb**	**Λ-Yb**
4	0.134	-0.127	-0.030	0.033	-0.053	0.062	0.019	-0.014
30	0.115	-0.149	-0.024	0.030	-0.049	0.063	0.016	-0.018
80	0.094	-0.094	-0.007	0.010	-0.046	0.044	0.014	-0.011
150	0.078	-0.070	0.004	-0.005	-0.034	0.036	0.007	-0.006
300	0.044	-0.039	0.017	-0.019	-0.020	0.017	-0.004	0.003

S 9. COMPUTATIONAL DETAILS

The multi-reference calculations were carried out with the OpenMolcas software package (version 19.11).[10] The static correlation was treated using the complete active space self-consistent field (CASSCF) approach.[11] The active space used corresponds to 13 electrons spanning the seven 4f orbitals of the Yb(III) ion. This active space was then augmented with the five unoccupied 5d orbitals of the Yb(III) ion. To do so, the additional 5d orbitals were first optimized within a RAS3 space by allowing single excitations at the RASSCF level, giving the following RAS[13,0,1,0,7,5] space. Using the optimized orbitals, double excitations from the RAS2 space constituted of the 4f orbitals were added at the RASCl level (RAS[13,0,2,0,7,5]). Using this RAS space, dynamic correlation was added at the PT2 level with a real shift of 0.65 to avoid intruder states.[12] In order to describe the low-lying 4f states, the state-average formalism was used with 7 SR spin-doublet states. The scalar relativistic (SR) effects were considered with the second-order Douglas-Kroll-Hess SR Hamiltonian.[13–16] In contrast to previous calculations, the Douglas-Kroll-Hess transformation at the second order have been also applied to calculate the integrals of the transition moments. Relativistic effects were also considered by using the all-electron atomic natural orbital relativistically contracted (ANO-RCC) basis set from the Molcas library.[17,18] The following contractions were used for Yb [25s22p15d11f4g2h/8s7p4d3f2g], O and N [14s9p4d3f2g/4s3p2d], C [14s9p4d3f2g/3s2p1d], and H [8s4p3d1f/2s]. The spin-orbit coupling was introduced within a state interaction among the basis of the calculated SR spin-doublets using the restricted active space state interaction (RASSI) approach and the atomic mean-field integrals (AMFI) approximation.[19,20] Cholesky decomposition of the bi-electronic integrals was employed to save disk space and to speed up the calculations.[21] The resulting simulated CPL spectra were obtained as the sums of Gaussian functions (with the root mean square width of σ = 0.005 eV) centered at the vertical excitation energies. All calculations were done on the model shown in Figure S24. [7]

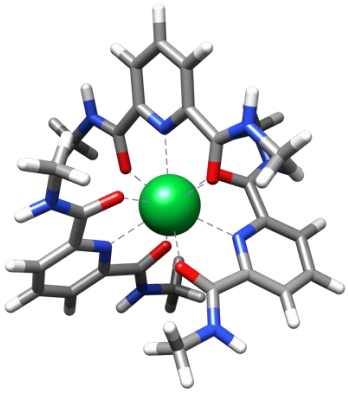

Figure S27. *Model of [Yb(R,R-L^{NHex2})$_3$(OTf)$_3$] / **Λ-Yb** used for the calculations. Color codes: green, Yb; red, O; blue, N; gray, C; white, H.*

Table S5: *Boltzmann population in percentage of the m_J composing the emissive $^2F_{5/2}$ term at various temperatures at SA-RAS[13,0,2,0,7,5]CI-PT2/RASSI-SO level of theory.*

Kramers doublets	0 K	30 K	80 K	150 K	300 K
2’	0	0	0.4	4.2	13.1
1’	0	0.8	14.2	26.6	33.2
0’	100	99.2	85.4	69.3	53.6

Table S6: *Calculated rotatory strength and oscillator strength of the electric dipole, magnetic dipole and electric quadrupole transition moments for all transitions $^2F_{5/2}\rightarrow{}^2F_{7/2}$ at SA-RAS[13,0,2,0,7,5]PT2/RASSI-SO level of theory.*

		E (cm-1)	*R* (cgs) / 10^{-40}	f_{ED}	f_{MD}	f_{EQ}
2'	⟶ 3	10735	-1.32E-1	9.69E-08	1.68E-07	2.68E-13
2'	⟶ 2	10940	6.92E-2	1.14E-06	3.74E-08	1.24E-12
2'	⟶ 1	10989	1.05E-1	1.42E-06	4.29E-08	1.05E-12
2'	⟶ 0	11126	-2.26E-1	4.42E-06	2.04E-08	1.20E-12
1'	⟶ 3	10541	1.43E-1	3.01E-06	3.48E-08	1.23E-12
1'	⟶ 2	10746	-1.72E-1	2.40E-06	1.22E-07	6.62E-13
1'	⟶ 1	10795	-2.19E-1	5.15E-06	6.55E-08	7.26E-13
1'	⟶ 0	10932	3.65E-1	2.77E-06	3.62E-08	6.34E-13
0'	⟶ 3	10441	-3.70E-2	7.63E-07	3.33E-08	1.25E-12
0'	⟶ 2	10646	3.54E-3	3.19E-06	4.28E-08	9.70E-13
0'	⟶ 1	10695	-7.65E-2	3.12E-06	7.63E-08	8.74E-13
0'	⟶ 0	10832	1.67E-1	8.29E-06	9.34E-08	4.30E-13

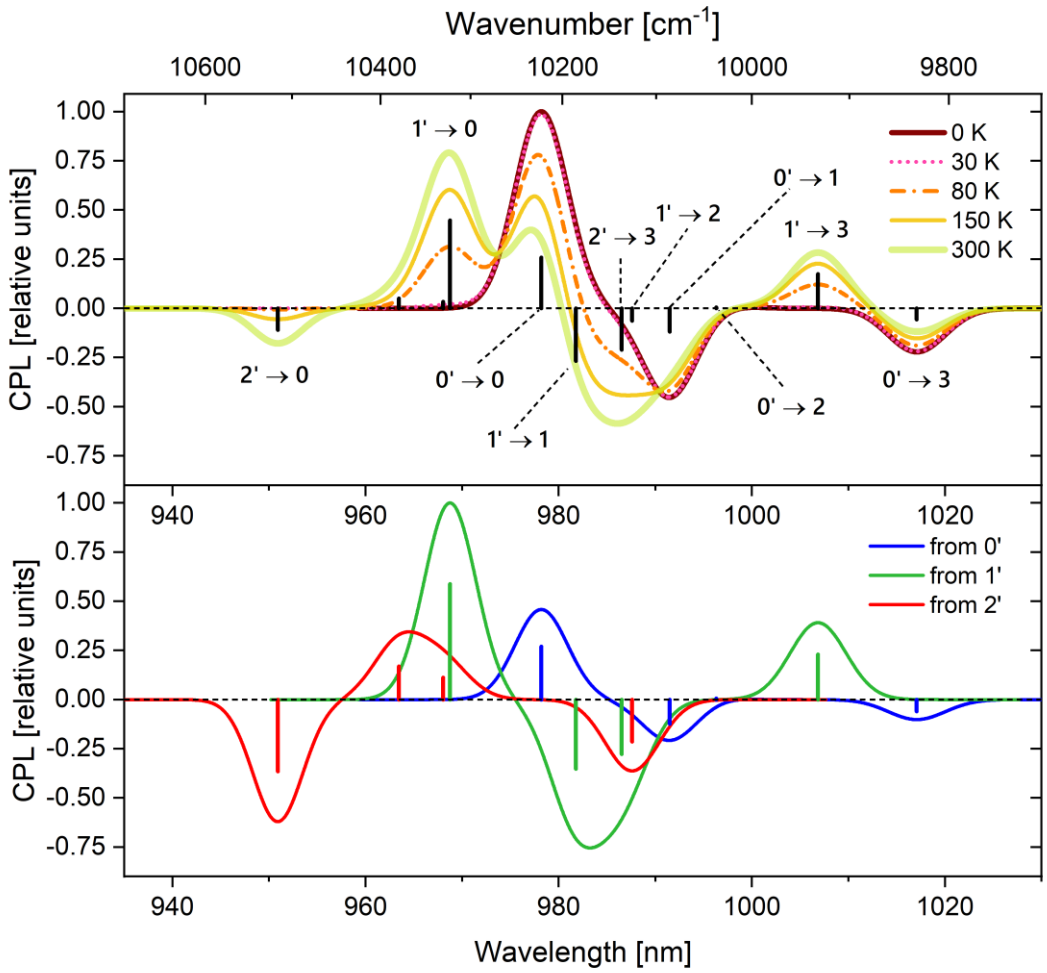

Figure S28: *Simulated CPL spectra of* ***Λ-Yb*** *as a function of the temperature (top) and with different absolute contributions of the emissive* $m_{J'}$ *(bottom). Calculations performed at SA-RAS[13,0,2,0,7,5]CI-PT2/RASSI-SO. Calculated rotatory strengths indicated as "stick" spectrum. An energetic shift of 610* cm^{-1} *has been applied to align the 0′ → 0 transition with the experimental one.*

References

1 G. M. Sheldrick, *Acta Crystallogr. Sect. Found. Adv.*, 2015, **71**, 3–8.
2 G. M. Sheldrick, *Acta Crystallogr. Sect. C Struct. Chem.*, 2015, **71**, 3–8.
3 A. L. Spek, *J. Appl. Crystallogr.*, 2003, **36**, 7–13.
4 A. F. Drake, *J. Phys. [E]*, 1986, **19**, 170.
5 L. Guy, M. Mosser, D. Pitrat, J.-C. Mulatier, M. Kukułka, M. Srebro-Hooper, E. Jeanneau, A. Bensalah-Ledoux, B. Baguenard and S. Guy, *J. Org. Chem.*, 2019, **84**, 10870–10876.
6 S. Guy, A. Bensalah-Ledoux, A. Lambert, Y. Guillin, L. Guy and J. C. Mulatier, *Thin Solid Films*, 2012, **520**, 6440–6445.
7 B. Baguenard, A. Bensalah-Ledoux, L. Guy, F. Riobé, O. Maury and S. Guy, *Nat. Commun.*, 2023, **14**, 1065.
8 F. Gendron, S. D. Pietro, L. Abad Galán, F. Riobé, V. Placide, L. Guy, F. Zinna, L. D. Bari, A. Bensalah-Ledoux, Y. Guyot, G. Pilet, F. Pointillart, B. Baguenard, S. Guy, O. Cador, O. Maury and B. Le Guennic, *Inorg. Chem. Front.*, 2021, **8**, 914–926.

9 M. G. Vivas, D. L. Silva, L. De Boni, Y. Bretonniere, C. Andraud, F. Laibe-Darbour, J.-C. Mulatier, R. Zaleśny, W. Bartkowiak, S. Canuto and C. R. Mendonca, *J. Phys. Chem. B*, 2012, **116**, 14677–14688.
10 I. Fdez. Galván, M. Vacher, A. Alavi, C. Angeli, F. Aquilante, J. Autschbach, J. J. Bao, S. I. Bokarev, N. A. Bogdanov, R. K. Carlson, L. F. Chibotaru, J. Creutzberg, N. Dattani, M. G. Delcey, S. S. Dong, A. Dreuw, L. Freitag, L. M. Frutos, L. Gagliardi, F. Gendron, A. Giussani, L. González, G. Grell, M. Guo, C. E. Hoyer, M. Johansson, S. Keller, S. Knecht, G. Kovačević, E. Källman, G. Li Manni, M. Lundberg, Y. Ma, S. Mai, J. P. Malhado, P. Å. Malmqvist, P. Marquetand, S. A. Mewes, J. Norell, M. Olivucci, M. Oppel, Q. M. Phung, K. Pierloot, F. Plasser, M. Reiher, A. M. Sand, I. Schapiro, P. Sharma, C. J. Stein, L. K. Sørensen, D. G. Truhlar, M. Ugandi, L. Ungur, A. Valentini, S. Vancoillie, V. Veryazov, O. Weser, T. A. Wesołowski, P.-O. Widmark, S. Wouters, A. Zech, J. P. Zobel and R. Lindh, *J. Chem. Theory Comput.*, 2019, **15**, 5925–5964.
11 B. O. Roos, P. R. Taylor and P. E. M. Sigbahn, *Chem. Phys.*, 1980, **48**, 157–173.
12 Kerstin. Andersson, P. Aake. Malmqvist, B. O. Roos, A. J. Sadlej and Krzysztof. Wolinski, *J. Phys. Chem.*, 1990, **94**, 5483–5488.
13 M. Douglas and N. M. Kroll, *Ann. Phys.*, 1974, **82**, 89–155.
14 B. A. Hess, *Phys. Rev. A*, 1985, **32**, 756–763.
15 B. A. Hess, *Phys. Rev. A*, 1986, **33**, 3742–3748.
16 A. Wolf, M. Reiher and B. A. Hess, *J. Chem. Phys.*, 2002, **117**, 9215–9226.
17 P.-O. Widmark, P.-Å. Malmqvist and B. O. Roos, *Theor. Chim. Acta*, 1990, **77**, 291–306.
18 B. O. Roos, R. Lindh, P.-Å. Malmqvist, V. Veryazov and P.-O. Widmark, *J. Phys. Chem. A*, 2004, **108**, 2851–2858.
19 P. Å. Malmqvist, B. O. Roos and B. Schimmelpfennig, *Chem. Phys. Lett.*, 2002, **357**, 230–240.
20 B. A. Heß, C. M. Marian, U. Wahlgren and O. Gropen, *Chem. Phys. Lett.*, 1996, **251**, 365–371.
21 F. Aquilante, R. Lindh and T. Bondo Pedersen, *J. Chem. Phys.*, 2007, **127**, 114107.